arXiv:hep-ph/0308146v1 13 Aug 2003

hep-ph/0308146

Improved full one–loop corrections to $A^0 \to \tilde{f}_1 \bar{\tilde{f}}_2$ and $\tilde{f}_2 \to \tilde{f}_1 A^0$

C. Weber, H. Eberl, W. Majerotto

Institut für Hochenergiephysik der Österreichischen Akademie der Wissenschaften, A–1050 Vienna, Austria

Abstract

We calculate the *full* electroweak one–loop corrections to the decay of the CP–odd Higgs boson A^0 into scalar fermions in the minimal supersymmetric extension of the Standard Model. For this purpose many parameters of the MSSM have to be properly renormalized in the on–shell renormalization scheme. We have also included the SUSY–QCD corrections. For the decay into bottom squarks and tau sleptons, especially for large $\tan\beta$, the corrections can be very large making the perturbation expansion unreliable. We solve this problem by an appropriate definition of the tree–level coupling in terms of running fermion masses and running trilinear couplings A_f. We also discuss the decay of heavy scalar fermions into light scalar fermions and A^0. We find that the corrections can be sizeable and therefore cannot be neglected.

1 Introduction

The search for a Higgs boson is the primary goal of all present and future high energy experiments at the TEVATRON, LHC or an e^+e^- Linear Collider. Whereas the Standard Model (SM) predicts just one Higgs boson, with the present lower bound of its mass $m_H \geq 114.4$ GeV (at 95% confidence level) [1], extensions of the SM allow for more Higgs bosons. In particular, the Minimal Supersymmetric Standard Model (MSSM) contains five physical Higgs bosons: two neutral CP–even (h^0 and H^0), one neutral CP–odd (A^0), and two charged ones ($H^\pm$) [2, 3]. The existence of a charged Higgs boson or a CP–odd neutral one would give clear evidence for physics beyond the SM. For a discovery precise predictions for its decay modes and their branching ratios are necessary. In case supersymmetric (SUSY) particles are not too heavy, the Higgs bosons can also decay into SUSY particles (neutralinos $\tilde{\chi}^0_i$, charginos $\tilde{\chi}^\pm_k$, sfermions $\tilde{f}_m$), $H^0, A^0 \to \tilde{\chi}^0_i \tilde{\chi}^0_j$ $(i,j = 1\ldots 4)$, $H^0, A^0 \to \tilde{\chi}^+_k \tilde{\chi}^-_l$ $(k,l = 1,\, 2)$, $H^0, A^0 \to \tilde{f}_m \bar{\tilde{f}}_n$ $(m,n = 1,\, 2)$, $H^\pm \to \tilde{\chi}^+_k \tilde{\chi}^0_i$, $H^\pm \to \tilde{f}_m \bar{\tilde{f}}'_n$. At tree–level, these decays were studied in [4, 5]. In particular, the branching ratios for the decays into sfermions, $H^0, A^0 \to \tilde{f}_m \bar{\tilde{f}}_n$, can be sizeable depending on the parameter space [6, 7]. The SUSY–QCD corrections to the decays into sfermions have also been calculated [8, 9]. The corrections to the decays into neutralinos [10] or charginos [11] due to fermion/sfermion exchanges have also been found non–negligible.

In this paper, we study in detail the decay of the CP–odd Higgs boson A^0 into two sfermions, $A^0 \to \tilde{f}_1 \bar{\tilde{f}}_2$. In particular, the third generation sfermions $\tilde{t}_i, \tilde{b}_i$, and $\tilde{\tau}_i$ are interesting because one expects them to be lighter than the other sfermions due to their large Yukawa couplings and left–right mixings. Since A^0 only couples to $\tilde{f}_L$–$\tilde{f}_R$ (left–right states of $\tilde{f}$), and due to the CP nature of A^0, $A^0 \to \tilde{f}_i \bar{\tilde{f}}_i$ vanishes. (This is valid also beyond tree–level for real parameters in the MSSM.) We will calculate the *full* electroweak corrections in the on–shell scheme. Owing to the fact that almost all parameters of the MSSM have to be renormalized in this process and hence a large number of graphs has to be computed, the calculation is very complex. Despite this complexity, we have performed the calculation in an analytic way. We have also studied the crossed channel $\tilde{f}_2 \to \tilde{f}_1 A^0$. Some important numerical results, especially for the decays of A^0 into the third generation squarks and the corresponding crossed channels have already been shown in [12].

This paper has three new elements. First, we give in the Appendix all analytical formulae needed for the calculation. Second, we describe in detail our method for improving the full one–loop calculation. As pointed out in [12], in the case of the decay of $A^0 \to \tilde{b}_1 \bar{\tilde{b}}_2$ or $A^0 \to \tilde{\tau}_1 \bar{\tilde{\tau}}_2$ the decay widths can receive large corrections, especially for large $\tan\beta$. This makes the perturbation expansion unreliable. In some cases the width can even become negative in the on–shell renormalization scheme. We present here a detailed description how this problem can be solved by an appropriate definition of the tree–level coupling in terms of running fermion masses and running trilinear coupling A_f $(f = b, \tau)$. For consistency between the on–shell and the $\overline{\rm DR}$ running parameters an iteration procedure is necessary. Moreover, in addition to the numerical results shown in [12] we present here new results for $A^0 \to \tilde{t}_1 \bar{\tilde{t}}_2$, $A^0 \to \tilde{b}_1 \bar{\tilde{b}}_2$, $A^0 \to \tilde{\tau}_1 \bar{\tilde{\tau}}_2$ and the corresponding crossed

channels.

The paper is organized as follows. In section 2 we summarize the tree–level formulae. In section 3 the full electroweak corrections are presented for which the explicit analytic formulae are given in the Appendices B, C, D. In section 4 a detailed description of the method to improve the one–loop calculation is presented. In section 5 the numerical treatment as well as numerical results are shown. Section 6 summarizes our conclusions.

2 Tree–level result

The sfermion mixing is described by the sfermion mass matrix in the left–right basis $(\tilde{f}_L, \tilde{f}_R)$, and in the mass basis $(\tilde{f}_1, \tilde{f}_2)$, $\tilde{f} = \tilde{t}, \tilde{b}$ or $\tilde{\tau}$,

$$\mathcal{M}^2_{\tilde{f}} = \begin{pmatrix} m^2_{\tilde{f}_L} & a_f\, m_f \\ a_f\, m_f & m^2_{\tilde{f}_R} \end{pmatrix} = \left(R^{\tilde{f}}\right)^\dagger \begin{pmatrix} m^2_{\tilde{f}_1} & 0 \\ 0 & m^2_{\tilde{f}_2} \end{pmatrix} R^{\tilde{f}}\,, \tag{1}$$

where $R^{\tilde{f}}_{i\alpha}$ is a 2 x 2 rotation matrix with rotation angle $\theta_{\tilde{f}}$, which relates the mass eigenstates $\tilde{f}_i$, $i = 1, 2$, $(m_{\tilde{f}_1} < m_{\tilde{f}_2})$ to the gauge eigenstates $\tilde{f}_\alpha$, $\alpha = L, R$, by $\tilde{f}_i = R^{\tilde{f}}_{i\alpha}\tilde{f}_\alpha$ and

$$m^2_{\tilde{f}_L} = M^2_{\{\tilde{Q},\tilde{L}\}} + (I^{3L}_f - e_f \sin^2\theta_W)\cos 2\beta\, m_Z^2 + m_f^2\,, \tag{2}$$

$$m^2_{\tilde{f}_R} = M^2_{\{\tilde{U},\tilde{D},\tilde{E}\}} + e_f \sin^2\theta_W \cos 2\beta\, m_Z^2 + m_f^2\,, \tag{3}$$

$$a_f = A_f - \mu\,(\tan\beta)^{-2I^{3L}_f}\,. \tag{4}$$

$M_{\tilde{Q}}$, $M_{\tilde{L}}$, $M_{\tilde{U}}$, $M_{\tilde{D}}$ and $M_{\tilde{E}}$ are soft SUSY breaking masses, A_f is the trilinear scalar coupling parameter, μ the higgsino mass parameter, $\tan\beta = \frac{v_2}{v_1}$ is the ratio of the vacuum expectation values of the two neutral Higgs doublet states [2, 3], I^{3L}_f denotes the third component of the weak isospin of the fermion f, e_f the electric charge in terms of the elementary charge e_0, and θ_W is the Weinberg angle.
The mass eigenvalues and the mixing angle in terms of primary parameters are

$$m^2_{\tilde{f}_{1,2}} = \frac{1}{2}\left(m^2_{\tilde{f}_L} + m^2_{\tilde{f}_R} \mp \sqrt{(m^2_{\tilde{f}_L} - m^2_{\tilde{f}_R})^2 + 4a_f^2 m_f^2}\right)\,, \tag{5}$$

$$\cos\theta_{\tilde{f}} = \frac{-a_f\, m_f}{\sqrt{(m^2_{\tilde{f}_L} - m^2_{\tilde{f}_1})^2 + a_f^2 m_f^2}} \qquad (0 \le \theta_{\tilde{f}} < \pi)\,, \tag{6}$$

and the trilinear breaking parameter A_f can be written as

$$m_f A_f = m^2_{LR} + m_f\,\mu\,(\tan\beta)^{-2I^{3L}_f} \tag{7}$$

with $m^2_{LR} \equiv (m^2_{\tilde{f}_1} - m^2_{\tilde{f}_2})\sin\theta_{\tilde{f}}\cos\theta_{\tilde{f}}$.
At tree–level the decay width of $A^0 \to \tilde{f}_1\bar{\tilde{f}}_2$ is given by

$$\Gamma^{\rm tree}(A^0 \to \tilde{f}_1\bar{\tilde{f}}_2) = \frac{N_C^f\,\kappa(m^2_{A^0}, m^2_{\tilde{f}_1}, m^2_{\tilde{f}_2})}{16\,\pi\, m^3_{A^0}}\,|G^{\tilde{f}}_{123}|^2 \tag{8}$$

with $\kappa(x,y,z) = \sqrt{(x-y-z)^2-4yz}$ and the colour factor $N_C^f = 3$ for squarks and $N_C^f = 1$ for sleptons, respectively. $G^{\tilde{f}}_{ij3}$ denotes the A^0–$\tilde{f}_i^*$–$\tilde{f}_j$ coupling as given in Appendix A.

3 Full Electroweak Corrections

The full one–loop corrected decay width is given by

$$\Gamma(A^0 \to \tilde{f}_1 \bar{\tilde{f}}_2) \;=\; \frac{N_C^f\, \kappa(m_{A^0}^2, m_{\tilde{f}_1}^2, m_{\tilde{f}_2}^2)}{16\,\pi\, m_{A^0}^3} \left[|G^{\tilde{f}}_{123}|^2 + 2\mathrm{Re}\left(G^{\tilde{f}}_{123} \cdot \Delta G^{\tilde{f}}_{123} \right) \right] . \qquad (9)$$

The (UV finite) corrections $\Delta G^{\tilde{f}}_{123}$ consist of the vertex corrections $\delta G^{\tilde{f}(v)}_{123}$ (Fig. 12), wave–function corrections and the coupling counter term corrections $\delta G^{\tilde{f}(c)}_{123}$ owing to the shift from the bare to the on–shell values,

$$\Delta G^{\tilde{f}}_{123} \;=\; \delta G^{\tilde{f}(v)}_{123} \;+\; \delta G^{\tilde{f}(w)}_{123} \;+\; \delta G^{\tilde{f}(c)}_{123} . \qquad (10)$$

The renormalization procedure with the fixings of the counter terms is given in [12]. The explicit formulae of the vertex corrections $\delta G^{\tilde{f}(v)}_{123}$ as well as the various contributions to the wave–function corrections $\delta G^{\tilde{f}(w)}_{123}$,

$$\delta G^{\tilde{f}(w)}_{123} \;=\; \frac{1}{2} \Re \Big[\delta Z^{\tilde{f}}_{11} + \delta Z^{\tilde{f}}_{22} + \delta Z^{H}_{33} \Big] G^{\tilde{f}}_{123} , \qquad (11)$$

can be found in the Appendices B and C. For the explicit formulae of the self–energies needed for the calculation of the counter term correction, $\delta G^{\tilde{f}(c)}_{123}$ (see eq. (23) of [12]) , we refer to the Appendix D.
Due to the diagrams with photon exchange we also have to consider real photon emission corrections to cancel the infrared divergences (Fig. 12). Therefore the corrected (UV– and IR–convergent) decay width is

$$\Gamma^{\mathrm{corr}}(A^0 \to \tilde{f}_1 \bar{\tilde{f}}_2) \;\equiv\; \Gamma(A^0 \to \tilde{f}_1 \bar{\tilde{f}}_2) + \Gamma(A^0 \to \tilde{f}_1 \bar{\tilde{f}}_2\, \gamma) . \qquad (12)$$

Throughout the paper we use the SUSY invariant dimensional reduction ($\overline{\mathrm{DR}}$) as regularization scheme. For convenience we perform the calculation in the 't Hooft–Feynman gauge, $\xi = 1$.

4 Improvement of One–loop Corrections

It has already pointed out in [12] that in the case of bottom squarks and tau sleptons, especially for large $\tan\beta$ the corrections to the decay widths $A^0 \to \tilde{b}_1 \bar{\tilde{b}}_2$ and $A^0 \to \tilde{\tau}_1 \bar{\tilde{\tau}}_2$ can be very large in the on–shell renormalization scheme. If the corrections are negative, the one–loop corrected width can even become negative and therefore unphysical. Hence

the perturbation expansion around the on–shell tree–level is no longer reliable. It has been shown in [13, 14] that, in the case of the decays into bottom squarks, the source of these large corrections are mainly the counter terms for m_b and the trilinear coupling A_b, in particular the SUSY–QCD corrections. However, despite the absence of strong interactions for the decay into tau sleptons, the corrections become extremely large. We show that this problem can be solved by defining an appropriate tree–level in terms of running values for m_f and A_f. The expansion around this new tree–level then no longer suffers from bad convergence.

Correction to m_b

First we review the improvement of the perturbation expansion by using $\overline{\rm DR}$ running bottom quark masses, following [14, 15, 16].

If the Yukawa coupling h_b is given at tree–level in terms of the pole mass m_b, the one–loop corrections become very large due to gluon and gluino exchange contributions to the counter term δm_b. The large counter term caused by the gluon loop is absorbed by using SM 2–loop renormalization group equations in the $\overline{\rm MS}$ scheme [14, 15, 16]. Thus we obtain the SM running bottom $\hat{m}_b(Q)_{\rm SM}$:

$$\hat{m}_b(Q)^{\overline{\rm MS}}_{\rm SM} = \left(\frac{\hat{m}_b(Q)^{\overline{\rm MS}}_{\rm SM}}{\hat{m}_b(m_b)^{\overline{\rm MS}}_{\rm SM}} \right) \hat{m}_b(m_b)^{\overline{\rm MS}}_{\rm SM} \tag{13}$$

The ratio $\left(\hat{m}_b(Q)^{\overline{\rm MS}}_{\rm SM}/\hat{m}_b(m_b)^{\overline{\rm MS}}_{\rm SM}\right)$ can be expressed as

$$\frac{\hat{m}_b(Q)^{\overline{\rm MS}}_{\rm SM}}{\hat{m}_b(m_b)^{\overline{\rm MS}}_{\rm SM}} = \begin{cases} \dfrac{c_5(\alpha_s^{(2)}(Q)/\pi)}{c_5(\alpha_s^{(2)}(m_b)/\pi)} & (m_b < Q \leq m_t)\,, \\ \dfrac{c_6(\alpha_s^{(2)}(Q)/\pi)}{c_6(\alpha_s^{(2)}(m_t)/\pi)} \dfrac{c_5(\alpha_s^{(2)}(m_t)/\pi)}{c_5(\alpha_s^{(2)}(m_b)/\pi)} & (Q > m_t)\,, \end{cases}$$

where we have used the functions

$$\begin{aligned} c_5(x) &= \left(\frac{23}{6}x\right)^{\frac{12}{23}} (1 + 1.175x) && (m_b < Q \leq m_t)\,, \\ c_6(x) &= \left(\frac{7}{2}x\right)^{\frac{4}{7}} (1 + 1.398x) && (Q > m_t)\,, \end{aligned}$$

and the 2–loop RGEs for α_s [16],

$$\alpha_s^{(2)}(Q) = \frac{12\pi}{(33 - 2\,n_f) \ln \frac{Q^2}{\Lambda^2_{n_f}}} \left(1 - \frac{6(153 - 19\,n_f)}{(33 - 2\,n_f)^2} \frac{\ln \ln \frac{Q^2}{\Lambda^2_{n_f}}}{\ln \frac{Q^2}{\Lambda^2_{n_f}}} \right)\,, \tag{14}$$

with $n_f = 5$ or 6 for $m_b < Q \leq m_t$ or $Q > m_t$, respectively. For the SM $\overline{\rm DR}$ running bottom mass at the scale $Q = m_b$ we use the $\overline{\rm MS}$ equation

$$\hat{m}_b(m_b)^{\overline{\rm MS}}_{\rm SM} = m_b \left[1 + \frac{4}{3} \frac{\alpha_s^{(2)}(m_b)}{\pi} + K_q \left(\frac{\alpha_s^{(2)}(m_b)}{\pi} \right)^2 \right]^{-1}\,, \tag{15}$$

with $K_q = 12.4$ and then convert to $\overline{\rm DR}$ using one–loop running $\alpha_s(Q)$:

$$\hat{m}_b(Q)_{\rm SM} \;=\; \left(\frac{\hat{m}_b(Q)^{\overline{\rm MS}}_{\rm SM}}{\hat{m}_b(m_b)^{\overline{\rm MS}}_{\rm SM}}\right) \hat{m}_b(m_b)^{\overline{\rm MS}}_{\rm SM} \;-\; \frac{\alpha_s(Q)}{3\pi}\, m_b \tag{16}$$

In the MSSM, for large $\tan\beta$ the counter term to m_b can be very large due to the gluino–mediated graph [13, 17, 18]. Here we absorb the gluino contribution as well as the sizeable contributions from neutralino and chargino loops and the remaining electroweak self–energies into the Higgs–sfermion–sfermion tree–level coupling. In such a way we obtain the full $\overline{\rm DR}$ running bottom quark mass

$$\hat{m}_b(Q)_{\rm MSSM} \;=\; \hat{m}_b(Q)_{\rm SM} + \delta m_b(Q)\,. \tag{17}$$

The explicit form of the electroweak contribution to the counter term $\delta m_b(Q)$ is given in Appendix D.4.

Correction to $A_{b,\tau}$
The second source of a very large correction (in the on–shell scheme) are the counter terms for the trilinear coupling $A_{b,\tau}$, (see eq. 7),

$$\delta A_{b,\tau} \;=\; \frac{\delta m^2_{LR}}{m_{b,\tau}} \;-\; \frac{m^2_{LR}}{m_{b,\tau}}\,\frac{\delta m_{b,\tau}}{m_{b,\tau}} \;+\; \delta\mu\tan\beta \;+\; \mu\,\delta\tan\beta\,. \tag{18}$$

Again, the big bottom mass correction δm_b contributes to δA_b, but also the counter term of the left–right mixing elements of the sfermion mass matrix, δm^2_{LR}, gives a very large correction for higher values of $\tan\beta$. In particular, in the case of the decay into staus, this is the main source for the bad convergence of the tree–level expansion. As in the case of the large correction to m_b we redefine the Higgs–sfermion–sfermion tree–level coupling in terms of $\overline{\rm DR}$ running $\hat{A}_{b,\tau}(m_{A^0})$. Because of the fact that the counter terms $\delta A_{b,\tau}$ (for large $\tan\beta$) can become several orders of magnitude larger than the on–shell $A_{b,\tau}$ we use $\hat{A}_{b,\tau}(m_{A^0})$ as input [14]. In order to be consistent we have to perform an iteration procedure to get all the correct running and on–shell masses, mixing angles and other parameters. This procedure is described below.

5 Method of improvement

In this section we will explain in detail how we can improve the perturbation calculation for the sbottom and stau case by using $\overline{\rm DR}$ running values for m_b and $A_{b,\tau}$ in the Higgs–sfermion–sfermion tree–level couplings. Since we take $\overline{\rm DR}$ running values for $\hat{A}_b$ and $\hat{A}_\tau$ as input and all other parameters on–shell we will have to pay attention to the sbottom and stau sector in order to get consistently all needed running and on–shell masses, mixing angles and other parameters. Here we adopt the procedure developed in [14] and also extend it to the electroweak case.

5.1 Calculation of running and on–shell parameters

Stop sector:
We start our calculation in the stop sector. Because all input parameters in the stop sector are on–shell we obtain the on–shell masses $m_{\tilde{t}_1}$, $m_{\tilde{t}_2}$ and the stop mixing angle $\theta_{\tilde{t}}$ by diagonalizing the stop mass matrix in the $\tilde{t}_L$–$\tilde{t}_R$ basis, see chapter 2. The running stop masses $\hat{m}_{\tilde{t}_i}$ and mixing angle $\hat{\theta}_{\tilde{t}}$ are calculated at the scale $Q = Q_{\tilde{t}} = \sqrt{m_{\tilde{t}_1} m_{\tilde{t}_2}}$ by adding the appropriate counter terms to the on–shell values in

$$\hat{m}^2_{\tilde{t}_i}(Q_{\tilde{t}}) = m^2_{\tilde{t}_i} + \delta m^2_{\tilde{t}_i}\,, \tag{19}$$

$$\delta m^2_{\tilde{t}_i} = \Re\,\Pi^{\tilde{t}}_{ii}(m^2_{\tilde{t}_i})\,, \tag{20}$$

$$\hat{\theta}_{\tilde{t}}(Q_{\tilde{t}}) = \theta_{\tilde{t}} + \delta\theta_{\tilde{t}}\,. \tag{21}$$

The electroweak parts of the sfermion self–energies $\Pi^{\tilde{f}}_{ii}(m^2_{\tilde{f}_i})$ are given in Appendix D.6 and the SUSY–QCD contributions, $\Pi^{\rm SUSY-QCD}_{ii}(m^2_{\tilde{f}_i})$ are given in eqs. (25)–(27) in [8]. Here and in the following all running parameters $\hat{X}(Q)$ are related to their on–shell values X by $\hat{X}(Q) = X + \delta X$, with δX being the full one–loop counter term — also including the SUSY–QCD parts. The mixing angle is fixed by [19]

$$\delta\theta_{\tilde{f}} = \frac{1}{4}\left(\delta Z^{\tilde{f}}_{12} - \delta Z^{\tilde{f}}_{21}\right) = \frac{1}{2(m^2_{\tilde{f}_1} - m^2_{\tilde{f}_2})}\,{\rm Re}\left(\Pi^{\tilde{f}}_{12}(m^2_{\tilde{f}_2}) + \Pi^{\tilde{f}}_{21}(m^2_{\tilde{f}_1})\right)\,. \tag{22}$$

For $\overline{\rm DR}$ running $\hat{m}_t$ we use the formulae from section 4 with the obvious substitutions $m_b \to m_t$ and $K_q = 10.9$ for the top–case. Next we evaluate the running parameters $\hat{M}_{\tilde{Q}}(Q)$ and $\hat{M}_{\tilde{U}}(Q)$ by inserting the running values $\hat{m}^2_{\tilde{t}_i}(Q), \hat{\theta}_{\tilde{t}}(Q), \hat{m}_t(Q)_{\rm MSSM}$, $\hat{m}_Z(Q) = m_Z + \delta m_Z$, $\hat{\beta}(Q) = \beta + \delta\beta$ and $\hat{\theta}_W = \theta_W - \frac{1}{\sin\theta_W}\left(\frac{\delta m_W}{m_W} - \frac{\delta m_Z}{m_Z}\right)$ into the equations

$$M^2_{\tilde{Q}} = m^2_{\tilde{t}_1}\cos^2\theta_{\tilde{t}} + m^2_{\tilde{t}_2}\sin^2\theta_{\tilde{t}} - m^2_t - m^2_Z\cos 2\beta\left(I^{3L}_t - e_t\sin^2\theta_W\right)\,, \tag{23}$$

$$M^2_{\tilde{U}} = m^2_{\tilde{t}_1}\sin^2\theta_{\tilde{t}} + m^2_{\tilde{t}_2}\cos^2\theta_{\tilde{t}} - m^2_t - m^2_Z\cos 2\beta\, e_t\sin^2\theta_W\,. \tag{24}$$

For the running value of A_t we use (see eq. (7))

$$\hat{A}_t = (\hat{m}^2_{\tilde{t}_1} - \hat{m}^2_{\tilde{t}_2})\,\frac{\sin 2\hat{\theta}_{\tilde{t}}}{\hat{m}_t} + \hat{\mu}\,\cot\hat{\beta}\,, \tag{25}$$

where we have taken running $\hat{\mu}(Q) = \mu + (\delta X)_{22}$ [20, 21].

Sbottom sector:
In the sbottom sector we have given all parameters on–shell except the parameter for the trilinear coupling, $\hat{A}_b(Q)$, which is running. First we calculate $\hat{m}_b(Q_{\tilde{b}})_{\rm MSSM}$ from eq. (17) at the scale $Q_{\tilde{b}} = \sqrt{m_{\tilde{b}_1} m_{\tilde{b}_2}}$. From the stop sector we already know the running values of $M_{\tilde{Q}}, \tan\beta$ and μ. Then we diagonalize the sbottom mass matrix using $\hat{m}_b(Q_{\tilde{b}})_{\rm MSSM}, \hat{M}_{\tilde{Q}}, \tan\hat{\beta}, \hat{\mu}$ and on–shell $M_{\tilde{D}}$, which is near its running value $\hat{M}_{\tilde{D}}$, to obtain the starting values for $\hat{m}_{\tilde{b}_i}$ and $\hat{\theta}_{\tilde{b}}$. The on–shell sbottom masses $m_{\tilde{b}_i}$ and the mixing

angle $\theta_{\tilde{b}}$ are calculated from their running values by subtracting the appropriate counter terms, i. e. $m^2_{\tilde{b}_i} = \hat{m}^2_{\tilde{b}_i}(Q) - \delta m^2_{\tilde{b}_i}$, $\theta_{\tilde{b}} = \hat{\theta}_{\tilde{b}}(Q) - \delta\theta_{\tilde{b}}$. Now we can compute the running value for $M_{\tilde{D}}$. Using the relation (see eq. (3))

$$M^2_{\tilde{D}} \;=\; m^2_{\tilde{b}_1}\sin^2\theta_{\tilde{b}} + m^2_{\tilde{b}_2}\cos^2\theta_{\tilde{b}} - m^2_b - m^2_Z\cos 2\beta\, e_b \sin^2\theta_W \tag{26}$$

we get $\hat{M}_{\tilde{D}} = (M^2_{\tilde{D}} + \delta M^2_{\tilde{D}})^{1/2} \approx M_{\tilde{D}} + \delta M^2_{\tilde{D}}/(2M_{\tilde{D}})$ with

$$\begin{aligned}\delta M^2_{\tilde{D}} \;=\;& \delta m^2_{\tilde{b}_1}\sin^2\theta_{\tilde{b}} + \delta m^2_{\tilde{b}_2}\cos^2\theta_{\tilde{b}} + \left(m^2_{\tilde{b}_1} - m^2_{\tilde{b}_2}\right)\sin 2\theta_{\tilde{b}}\,\delta\theta_{\tilde{b}} - 2m_b\,\delta m_b \\ & -\delta m^2_Z\cos 2\beta\, e_b\sin^2\theta_W + 2m^2_Z\sin 2\beta\,\delta\beta\, e_b\sin^2\theta_W - m^2_Z\cos 2\beta\, e_b\,\delta\sin^2\theta_W\end{aligned} \tag{27}$$

and $\delta m_b = \hat{m}_b(Q_{\tilde{b}})_{\rm MSSM} - m_b$. Because the parameters involved in these calculations are very entangled, e. g. $\hat{M}_{\tilde{D}}$ depends on the $\delta m_{\tilde{b}_i}$ which themselves depend on $M_{\tilde{D}}$, we have to perform an iteration procedure.

Iteration procedure:
Here we will describe in detail the procedure how we obtain all necessary on–shell and running parameters. For convenience, we shortly denote all masses, parameters, couplings etc. for a certain $n \geq 1$ in the iteration by $\hat{\mathcal{X}}^{(n)}$. As starting values $\hat{\mathcal{X}}^{(0)}$ we take on–shell masses and parameters (except $\hat{A}_b$ which is running) and the couplings derived from these quantities. The only exceptions are the standard model running fermion masses $\hat{m}^{(0)}_f = \hat{m}_f(Q)_{\rm SM}$. $\hat{m}_f$ shortly stands for the full $\overline{\rm DR}$ running fermion masses, $\hat{m}_f(Q)_{\rm MSSM}$. The single steps of the iteration procedure are the following:

1. The running stop masses and the stop mixing angle are calculated as explained above by $\hat{m}^{2\,(n)}_{\tilde{t}_i} = m^2_{\tilde{t}_i} + \delta m^{2\,(n)}_{\tilde{t}_i}(\hat{\mathcal{X}}^{(n-1)})$ and $\hat{\theta}^{(n)}_{\tilde{t}} = \theta_{\tilde{t}} + \delta\theta^{(n)}_{\tilde{t}}(\hat{\mathcal{X}}^{(n-1)})$.

2. $\hat{m}^{(n)}_t = \hat{m}_{t,\rm SM} + \delta m^{(n)}_t(\hat{\mathcal{X}}^{(n-1)})$

3. $\hat{m}^{(n)}_Z = m_Z + \delta m^{(n)}_Z(\hat{\mathcal{X}}^{(n-1)})$ and
   $\sin^2\hat{\theta}^{(n)}_W = \sin^2\theta_W + \delta\sin^2\theta^{(n)}_W$ with $\delta\sin^2\theta^{(n)}_W = -\cos^2\theta_W\left(\dfrac{\delta m_W}{m_W} - \dfrac{\delta m_Z}{m_Z}\right)(\hat{\mathcal{X}}^{(n-1)})$

4. The running value of $\tan\beta$, $\tan\hat{\beta}^{(n)} = \tan\beta + \delta\tan\beta^{(n)}$,
   with $\delta\tan\beta^{(n)} = \dfrac{1}{m_Z\sin 2\beta}\,{\rm Im}\Pi_{A^0Z^0}(\hat{\mathcal{X}}^{(n-1)})\tan\beta$ [22].

5. $\hat{\mu}^{(n)} = \mu + \delta\mu^{(n)}$ with $\delta\mu^{(n)} = \delta X_{22}(\hat{\mathcal{X}}^{(n-1)})$.

6. The soft SUSY breaking masses $\hat{M}^{(n)}_{\tilde{Q},\tilde{U}}$ are calculated from $\hat{m}^{(n)}_{\tilde{t}_i}$, $\hat{\theta}^{(n)}_{\tilde{t}}$, $\hat{m}_t(Q_{\tilde{t}})^{(n)}$, $\hat{m}^{(n)}_Z$, $\sin^2\hat{\theta}^{(n)}_W$ and $\tan\hat{\beta}^{(n)}$.

7. We compute the running $\hat{A}_t$ by using running values in eq. (25):
   $\hat{A}^{(n)}_t = \left(\hat{m}^{2\,(n)}_{\tilde{t}_1} - m^{2\,(n)}_{\tilde{t}_2}\right)\dfrac{\sin 2\hat{\theta}^{(n)}_{\tilde{t}}}{\hat{m}^{(n)}_t} + \hat{\mu}^{(n)}\,\cot\hat{\beta}^{(n)}$

8. In the sbottom sector we obtain $\delta m_b^{(n)}$ from the running values already calculated in steps 1.–7., like $\hat{m}_{\tilde{b}_i}^{(n)}$, $\hat{\theta}_{\tilde{b}}^{(n)}$ or $\hat{m}_f^{(n)}$, and the remaining masses, couplings etc. from $\hat{\mathcal{X}}^{(n-1)}$.

9. $\hat{m}_b^{(n)} = \hat{m}_{b,\rm SM} + \delta m_b^{(n)}$.

10. We receive the running sbottom masses, $\hat{m}_{\tilde{b}_i}^{(n)}$, and the mixing angle, $\hat{\theta}_{\tilde{b}}^{(n)}$, by solving the mass eigenvalue problem with the running values of $\hat{M}_{\tilde{Q}}^{(n)}$, $\hat{M}_{\tilde{D}}^{(n-1)}$, $\hat{m}_b^{(n)}$, $\hat{A}_b$, $\hat{\mu}^{(n)}$ and $\tan\hat{\beta}^{(n)}$.

11. The on–shell sbottom masses $m_{\tilde{b}_i}^{2\,(n)} = \hat{m}_{\tilde{b}_i}^{2\,(n)} - \delta m_{\tilde{b}_i}^{2\,(n)}(Q_{\tilde{b}}^{(n)})$ at the scale $Q_{\tilde{b}}^{(n)} = \sqrt{\hat{m}_{\tilde{b}_1}^{(n)}\hat{m}_{\tilde{b}_2}^{(n)}}$, and $\theta_{\tilde{b}}^{(n)} = \hat{\theta}_{\tilde{b}}^{(n)} - \delta\theta_{\tilde{b}}^{(n)}$.

12. $$\begin{aligned}\delta M_{\tilde{D}}^{2\,(n)} \;=\; & \delta m_{\tilde{b}_1}^{2\,(n)}\sin^2\theta_{\tilde{b}} + \delta m_{\tilde{b}_2}^{2\,(n)}\cos^2\theta_{\tilde{b}} + \left(m_{\tilde{b}_1}^2 - m_{\tilde{b}_2}^2\right)\sin 2\theta_{\tilde{b}}\,\delta\theta_{\tilde{b}}^{(n)} - 2m_b\left(\hat{m}_b^{(n)} - m_b\right) \\ & - \delta m_Z^{2\,(n)}\cos 2\beta\, e_b \sin^2\theta_W + 2m_Z^2 \sin 2\beta\,\delta\beta^{(n)}\, e_b \sin^2\theta_W - m_Z^2\cos 2\beta\, e_b\,\delta\sin^2\theta_W^{(n)}.\end{aligned}$$
(Remember that the values without a hat ($\hat{}$) are on–shell ones!)

13. $\hat{M}_{\tilde{D}}^{(n)} = M_{\tilde{D}} + \dfrac{1}{2}\dfrac{\delta M_{\tilde{D}}^{2\,(n)}}{M_{\tilde{D}}}$.

14. In the sneutrino sector we calculate the running sneutrino mass $\hat{m}_{\tilde{\nu}_\tau}^{2\,(n)} = m_{\tilde{\nu}_\tau}^2 + \delta m_{\tilde{\nu}_\tau}^{2\,(n)}(\hat{\mathcal{X}}^{(n-1)})$ and $\hat{M}_{\tilde{L}}^{2\,(n)} = \hat{m}_{\tilde{\nu}_\tau}^{2\,(n)} - \frac{1}{2}\,\hat{m}_Z^{(n)}\cos 2\hat{\beta}^{(n)}$, see also eq (23).

15. In the stau sector the values for running $\hat{m}_\tau^{(n)}, \hat{m}_{\tilde{\tau}_i}^{(n)}$ etc. are calculated like in the steps 8–13 in the sbottom sector with the evident substitution $\tilde{b} \to \tilde{\tau}$ for the corresponding parameters and $M_{\tilde{Q}} \to M_{\tilde{L}}, M_{\tilde{D}} \to M_{\tilde{E}}$.

16. All couplings are recalculated with the new running parameters $\to \hat{\mathcal{X}}^n$.

The iteration starts with $n = 1$ and ends, when certain parameters are calculated precisely enough for a given accuracy, i. e. $\left|1 - \frac{\hat{x}^{(n)}}{\hat{x}^{(n-1)}}\right| < \varepsilon$ for $\hat{x} = \{\hat{m}_b, \hat{M}_{\tilde{D}}, \hat{m}_\tau, \hat{M}_{\tilde{E}}\}$. For ε we choose $\varepsilon = 10^{-8}$. We have checked the consistency of this procedure by computing the on–shell $M_{\tilde{D}}$ and running $M_{\tilde{Q}}$ from the sbottom sector by using

$$M_{\tilde{D}}^2 \;=\; m_{\tilde{b}_1}^2\sin^2\theta_{\tilde{b}} + m_{\tilde{b}_2}^2\cos^2\theta_{\tilde{b}} - m_b^2 - m_Z^2\cos 2\beta\, e_b\sin^2\theta_W\,, \tag{28}$$

$$\hat{M}_{\tilde{Q}}^2 \;=\; \hat{m}_{\tilde{b}_1}^2\cos^2\hat{\theta}_{\tilde{b}} + \hat{m}_{\tilde{b}_2}^2\sin^2\hat{\theta}_{\tilde{b}} - \hat{m}_b^2 - \hat{m}_Z^2\cos 2\hat{\beta}\left(I_b^{3L} - e_b\sin^2\hat{\theta}_W\right)\,, \tag{29}$$

which are equal (up to higher order corrections) to the on–shell input $M_{\tilde{D}}$ and running $M_{\tilde{Q}}$ from the stop sector.
For easier reading the single steps of the iteration procedure of the stop and sbottom sector are depicted in the flowchart in Fig. 1.

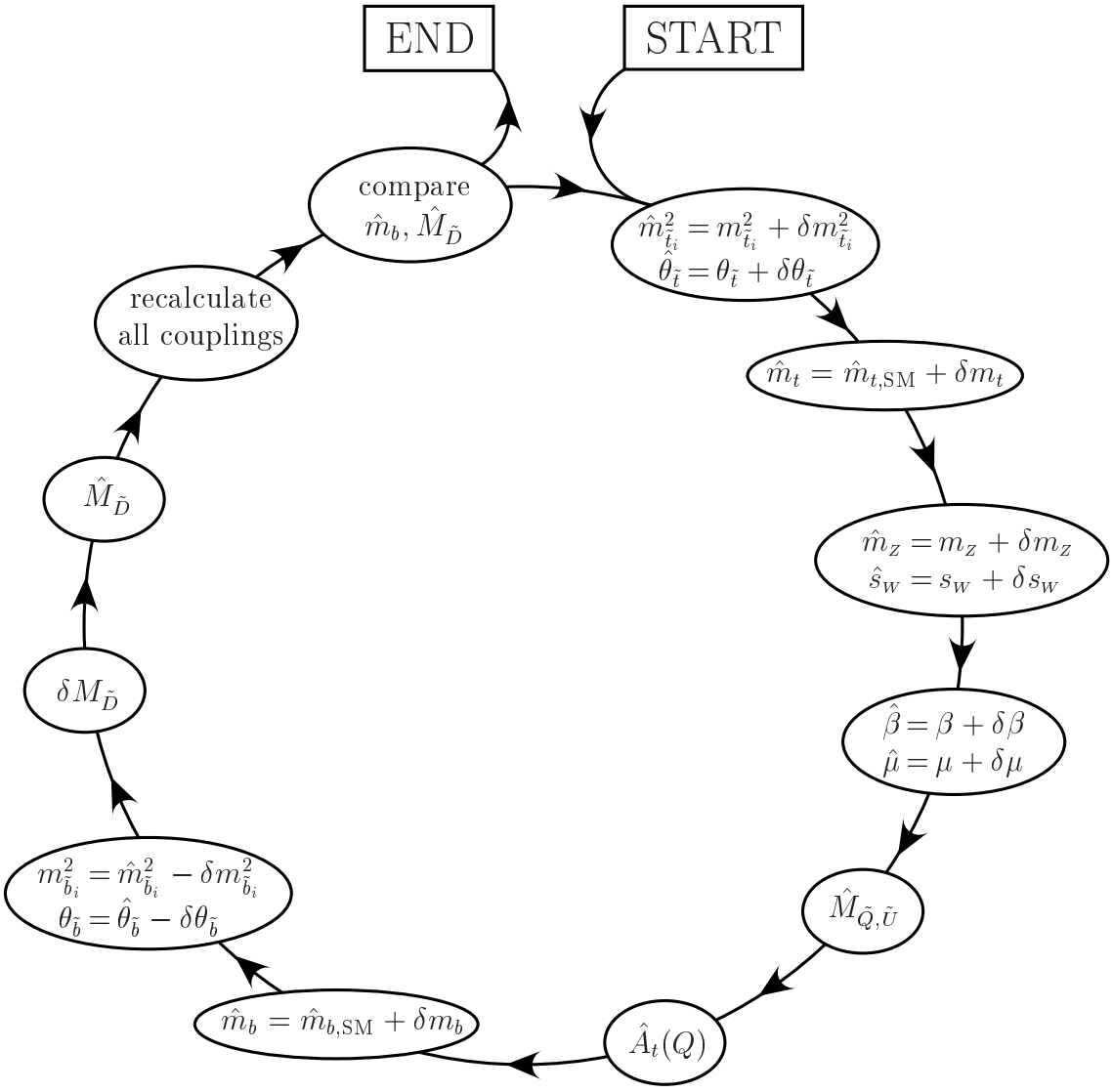

Figure 1: Simplified flowchart for the iteration procedure. For details see section 5.1.

5.2 Numerical results

In the following numerical examples, we take for the standard model parameters $m_Z = 91.1876$ GeV, $m_W = 80.423$ GeV, $\sin^2\theta_W = 1 - m_W^2/m_Z^2$, $\alpha(m_Z) = 1/127.934$, $m_t = 174.3$ GeV, $m_b = 4.7$ GeV, $m_\tau = 1.8$ GeV and $\{m_u, m_d, m_e, m_c, m_s, m_\mu\} = \{4, 8, 0.511, 1300, 200, 106\}$ MeV for 1st and 2nd generation fermions. M' is fixed by the gaugino unification relation $M' = \frac{5}{3}\tan^2\theta_W M$, therefore the gluino mass is related to M by $m_{\tilde{g}} = (\alpha_s(m_{\tilde{g}})/\alpha)\sin^2\theta_W M$. In order to reduce the number of parameters in the input parameter set, we assume $M_{\tilde{Q}} \equiv M_{\tilde{Q}_3} = \frac{10}{9}M_{\tilde{U}_3} = \frac{10}{11}M_{\tilde{D}_3} = M_{\tilde{L}_3} = M_{\tilde{E}_3} = M_{\tilde{Q}_{1,2}} = M_{\tilde{U}_{1,2}} = M_{\tilde{D}_{1,2}} = M_{\tilde{L}_{1,2}} = M_{\tilde{E}_{1,2}}$ for the first, second and third generation soft SUSY breaking masses as well as $A \equiv A_t = A_b = A_\tau$ for all (s)fermion generations, if not stated otherwise.

stop–case:

In Fig. 2 we show the tree–level and the corrected widths to $A^0 \to \tilde{t}_1\bar{\tilde{t}}_2$ for $\tan\beta = 15$ and $\{m_{A^0}, A, M, M_{\tilde{Q}}\} = \{700, -500, 120, 300\}$ GeV as a function of the higgsino mass parameter μ. The electroweak corrections are almost constant about -7%.
At $\mu \approx -242$ GeV one can identify the pseudo–threshold coming from $\tilde{t}_2 \to t\,\tilde{\chi}_4^0$.

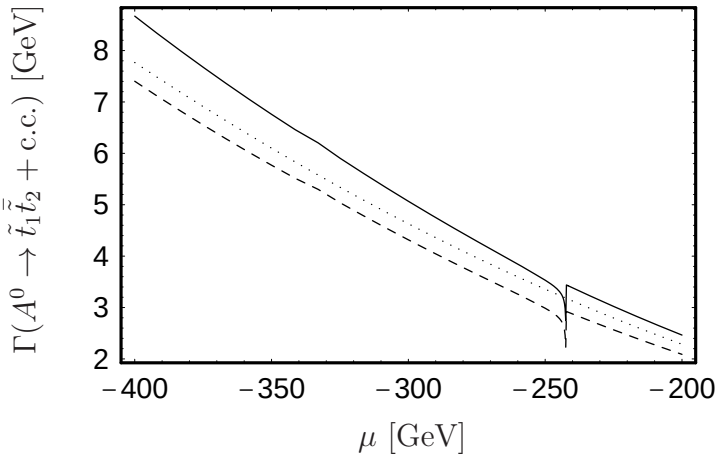

Figure 2: Tree–level (dotted line), full electroweak corrected decay width (dashed line) and full one–loop (electroweak and SUSY–QCD) corrected width (solid line) of $A^0 \to \tilde{t}_1\bar{\tilde{t}}_2$ as a function of μ.

Fig. 3 shows the tree–level, the full electroweak and the full one–loop corrected (electroweak and SUSY–QCD) decay width of $A^0 \to \tilde{t}_1\bar{\tilde{t}}_2$ as a function of the lighter stop mass, $m_{\tilde{t}_1}$, where $M_{\tilde{Q}}$ is varied from 200 to 450 GeV. As input parameters we choose $\{m_{A^0}, \mu, A, M\} = \{900, 250, 300, 120\}$ GeV and $\tan\beta = 7$. Again, in a large region of the parameter space the electroweak corrections are comparable to the SUSY–QCD ones. The pseudo–threshold at $m_{\tilde{t}_1} \approx 304$ GeV originates from $\tilde{t}_2 \to t\,\tilde{\chi}_3^0$ in the wave–function correction.

In Fig. 4 the dependence of the crossed channel decay width, $\Gamma(\tilde{t}_2 \to \tilde{t}_1 A^0)$, as a

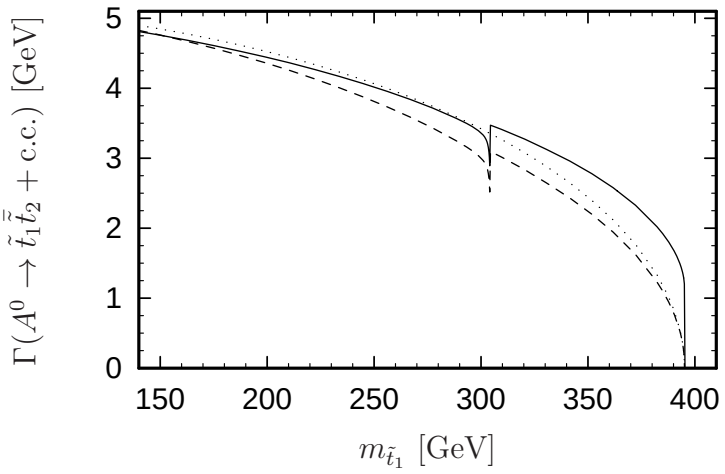

Figure 3: Tree–level (dotted line), full electroweak corrected decay width (dashed line) and full one–loop (electroweak and SUSY–QCD) corrected width (solid line) of $A^0 \to \tilde{t}_1 \bar{\tilde{t}}_2$ as a function of $m_{\tilde{t}_1}$.

function of $\tan\beta$ is given. We see that the electroweak corrections have different sign compared to the SUSY–QCD ones and go up to 10%. As input parameters we have chosen $\{m_{A^0}, \mu, A, M, M_{\tilde{Q}}\} = \{170, 500, -390, 250, 350\}$ GeV as well as $M_{\tilde{U}_3} = 450$ GeV to get an acceptable stop mass splitting.

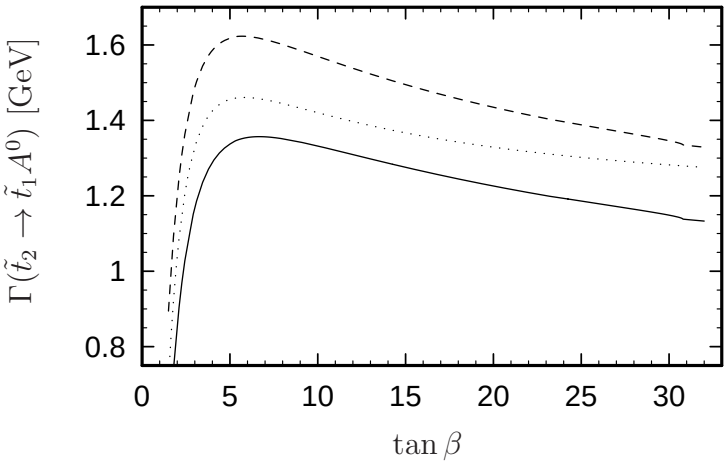

Figure 4: $\tan\beta$–dependence of the tree–level (dotted line), full electroweak corrected (dashed line) and full one–loop corrected (solid line) decay widths of $\tilde{t}_2 \to \tilde{t}_1 A^0$.

Fig. 5 shows the decay width $\Gamma(\tilde{t}_2 \to \tilde{t}_1 A^0)$ as a function of $m_{\tilde{t}_1}$, varying $M_{\tilde{Q}_3}$ from 200 to 460 GeV. To get a larger mass splitting for the top squarks, we relax the conditions for 3rd generation squarks and take $\{M_{\tilde{U}_3}, M_{\tilde{D}_3}\} = \{500, 300\}$ GeV. All other SUSY breaking masses are fixed at 300 GeV. For the remaining input parameters we choose $\{m_{A^0}, \mu, A\} = \{120, -400, -350\}$ GeV and $\tan\beta = 7$.

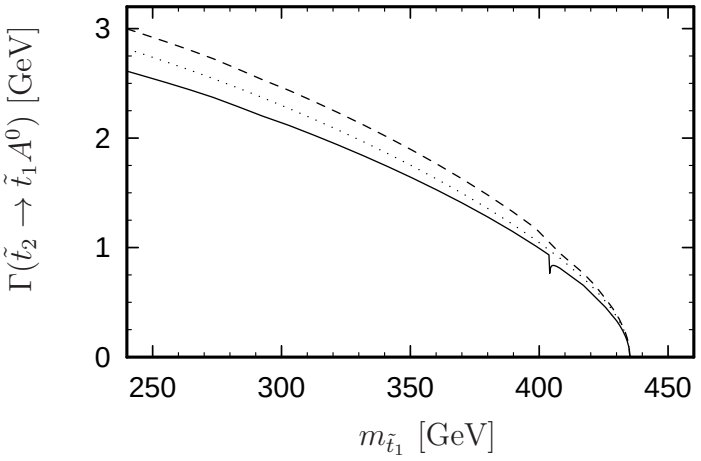

Figure 5: $m_{\tilde{t}_1}$–dependence of the tree–level (dotted line), full electroweak corrected (dashed line) and full one–loop corrected (solid line) decay widths of $\tilde{t}_2 \to \tilde{t}_1 A^0$.

sbottom–case:

In Fig. 6 we show two kinds of perturbation expansion for $\Gamma(A^0 \to \tilde{b}_1 \bar{\tilde{b}}_2)$ with $\{m_{A^0}, \mu, A, M, M_{\tilde{Q}}\} = \{800, -300, -500, 200, 300\}$ GeV: First we show the tree–level width, given in terms of on–shell input parameters (dotted line). The dashed and dash–dot–dotted line correspond to the on–shell electroweak and full (electroweak plus SUSY–QCD) one–loop width, respectively. For both corrections one can clearly see the invalidity of the on–shell perturbation expansion, which leads to an improper negative decay width. The second way of perturbation expansion is given by the dash–dotted and the solid line which correspond to the improved tree–level and improved full one–loop decay width,

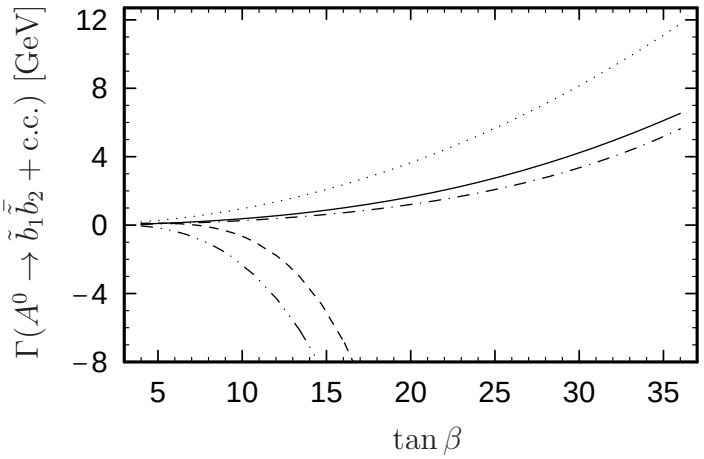

Figure 6: Two kinds of perturbation expansion: the dotted line corresponds to the on–shell tree–level width, the dashed and dash–dot–dotted line correspond to electroweak SUSY–QCD on–shell one–loop width, respectively. The dash–dotted line corresponds to improved the tree–level and the solid line to the (full) improved one–loop width.

respectively. Here we take the same input parameters as in the first case but with running $A = -500$ GeV.

In Fig. 7 we show the decay width $\Gamma(A^0 \to \tilde{b}_1 \bar{\tilde{b}}_2)$ as a function of $\overline{\rm DR}$ running A for $\{m_{A^0}, \mu, M, M_{\tilde{Q}}\} = \{800, -300, 300, 300\}$ GeV and $\tan\beta = 30$. The dotted line corresponds to the improved tree–level, the dashed line corresponds to the improved SUSY–QCD one–loop width and the solid line shows the full improved one–loop width. For negative A the electroweak corrections decrease the decay width by $\sim 20\%$, whereas for positive A the SUSY–QCD corrections almost vanish and the electroweak ones go up to 30%.

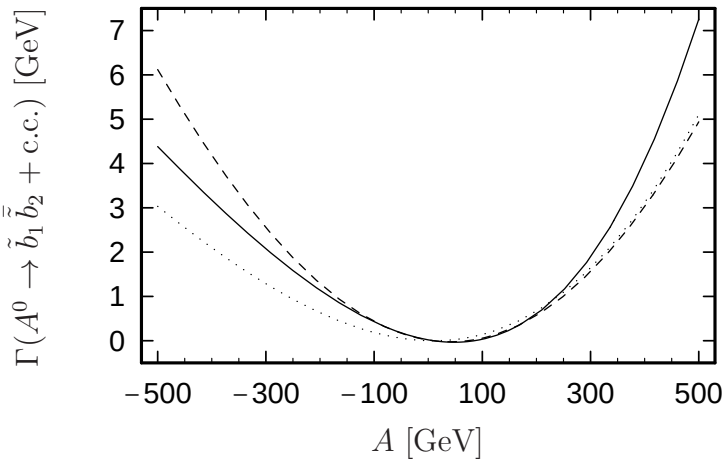

Figure 7: Perturbation expansion around the improved tree–level decay width (dotted line) of $\Gamma(A^0 \to \tilde{b}_1 \bar{\tilde{b}}_2)$ as a function of the trilinear coupling A. Dashed and solid lines correspond to the improved SUSY–QCD and full improved one–loop width, respectively.

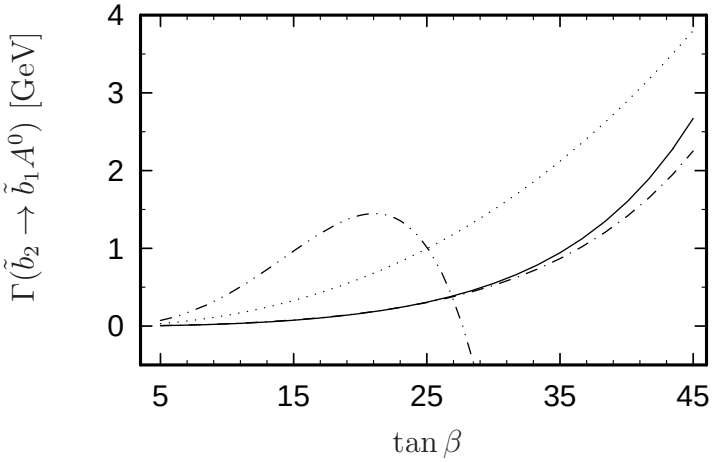

Figure 8: $\tan\beta$–dependence of $\Gamma(\tilde{b}_2 \to \tilde{b}_1 A^0)$ for two kinds of perturbation expansion. The dotted and dash–dot–dotted lines corresponds to on–shell tree–level and full one–loop width, respectively, the dash–dotted line corresponds to improved tree–level and the solid line shows the full improved one–loop width.

Fig. 8 shows the behaviour of the decay width $\Gamma(\tilde{b}_2 \to \tilde{b}_1 A^0)$ for large $\tan\beta$. As in Fig. 6 two kinds of perturbation expansion are given. The dotted and dash–dot–dotted lines correspond to the tree–level and full one–loop decay widths in the pure on–shell scheme. For large $\tan\beta$ one can clearly see the invalidity of the perturbation series, leading to a negative decay width. In the second case we show the expansion around the tree–level decay width, given in terms of running A_b and m_b. The dash–dotted line corresponds to the improved tree–level and the solid one to the one–loop width. Up to $\tan\beta \sim 30$ the corrections stay relatively small which indicates that already the (improved) tree–level is a good approximation for $\Gamma(\tilde{b}_2 \to \tilde{b}_1 A^0)$. As input parameters we take the values $\{m_{A^0}, \mu, A, M, M_{\tilde{Q}}\} = \{150, -220, 500, 200, 300\}$ GeV and $M_{\tilde{D}_3} = 500$ GeV for kinematical reasons.

In Fig. 9 the A^0 decay into two staus is given as a function of $\tan\beta$. Despite the absence of SUSY–QCD corrections the perturbation expansion around the on–shell tree–level (dotted line) leads to an improper negative decay width (dashed line) coming from large $\mathcal{O}(h_b^2)$ corrections. As input parameters we take $\{m_{A^0}, \mu, A, M, M_{\tilde{Q}}\} = \{800, 400, -500, 120, 300\}$ GeV. The dash–dotted line corresponds to the improved tree–level and the solid line shows the improved one–loop width for the same input parameters as above and running $A = -500$ GeV.

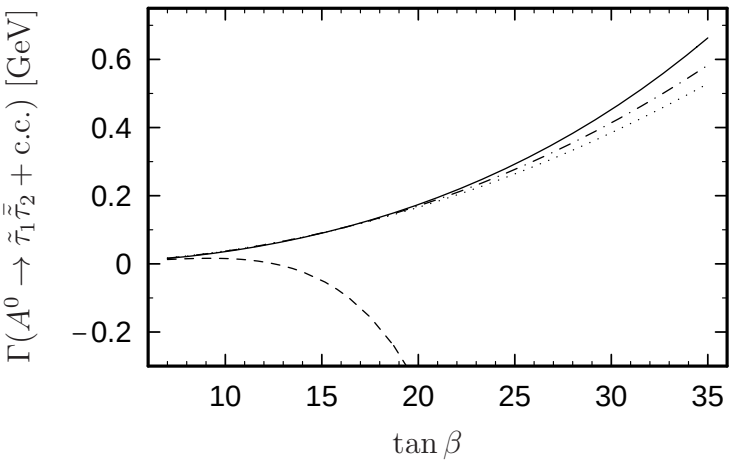

Figure 9: On–shell tree–level (dotted line) and full electroweak on–shell corrected decay width (dashed line) of $A^0 \to \tilde{\tau}_1 \bar{\tilde{\tau}}_2$ as a function of $\tan\beta$. The dash–dotted and solid lines correspond to improved tree–level and full improved one–loop decay widths.

Fig. 10 shows the decay width of $\Gamma(A^0 \to \tilde{\tau}_1 \bar{\tilde{\tau}}_2)$ as a function of the mass of the decaying Higgs boson A^0 for the improved perturbation expansion. The dotted and the solid lines correspond to the (improved) tree–level and full one–loop widths, respectively. In the whole region of the parameter space shown the (electroweak) corrections decrease the on–shell width by 15%. As input parameters we choose $\{\mu, A, M, M_{\tilde{Q}}\} = \{-450, -500, 120, 260\}$ GeV and $\tan\beta = 7$.

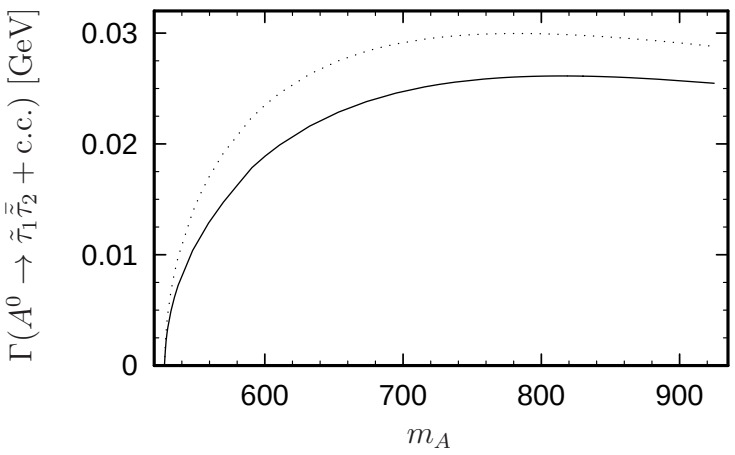

Figure 10: m_{A^0}–dependence of the improved tree–level (dotted line) and full one–loop corrected (solid line) decay widths of $\Gamma(A^0 \to \tilde{\tau}_1 \bar{\tilde{\tau}}_2)$.

In Fig. 11 we show the A dependence of $\Gamma(\tilde{\tau}_2 \to \tilde{\tau}_1 A^0)$ in the improved case. For negative values of A the corrections increase the on–shell width by $\sim 20\%$ whereas for positive values of A the corrections are negative and go up to 15%. The input parameters are taken as follows: $\{m_{A^0}, \mu, M, M_{\tilde{Q}}\} = \{150, 400, 300, 300\}$ GeV and $M_{\tilde{E}_3} = 500$ GeV for an acceptable stau mass splitting. For $\tan\beta$ we take the value 30.

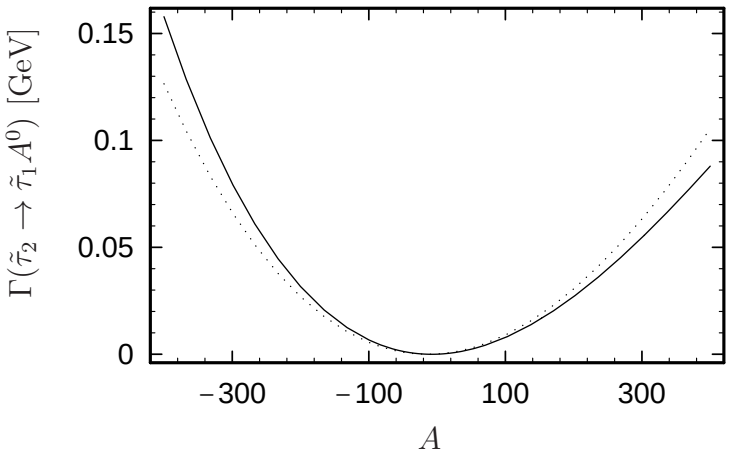

Figure 11: A–dependence of the improved tree–level (dotted line) and improved one–loop decay width (solid line) for $\tilde{\tau}_2 \to \tilde{\tau}_1 A^0$.

6 Conclusions

We have calculated the *full* electroweak one–loop corrections to the decay widths $A^0 \to \tilde{f}_1 \bar{\tilde{f}}_2$ and $\tilde{f}_2 \to \tilde{f}_1 A^0$ in the on–shell scheme. We have presented all formulae required for the computation. It has been necessary to renormalize almost all parameters of the MSSM. We have also included the SUSY–QCD corrections which were calculated in [8]. For the decay into bottom squarks and tau sleptons for large $\tan\beta$ an improvement of the on–shell perturbation expansion is necessary. We have worked out an iterative method to improve the one–loop calculation. Thereby, the tree–level coupling is redefined in terms of $\overline{\rm DR}$ running masses and running A_f. We find that the corrections are significant and in a wide range of the parameter space comparable to the SUSY–QCD corrections.

Acknowledgements
The authors acknowledge support from EU under the HPRN-CT-2000-00149 network programme and the "Fonds zur Förderung der wissenschaftlichen Forschung" of Austria, project No. P13139-PHY.

A Notation and Couplings

For the neutral and charged Higgs fields we use the notation $H_k^0 = \{h^0, H^0, A^0, G^0\}$, $H_k^+ = \{H^+, G^+, H^-, G^-\}$ and $H_k^- \equiv (H_k^+)^* = \{H^-, G^-, H^+, G^+\}$. $t/\tilde{t}$ stands for an up–type (s)fermion and $b/\tilde{b}$ for a down–type one. Following [2, 3] the Higgs–Sfermion–Sfermion couplings for neutral Higgs bosons, $G_{ijk}^{\tilde{f}}$, can be written as

$$G_{ijk}^{\tilde{f}} \;\equiv\; G\Big(H_k^0 \tilde{f}_i^* \tilde{f}_j\Big) = \Big[R^{\tilde{f}} G_{LR,k}^{\tilde{f}} (R^{\tilde{f}})^T\Big]_{ij}\,. \tag{30}$$

The 3rd generation left–right couplings $G_{LR,k}^{\tilde{f}}$ for up– and down–type sfermions are

$$\begin{aligned}
G_{LR,1}^{\tilde{t}} &= \begin{pmatrix} -\sqrt{2}h_t m_t c_\alpha + g_Z m_Z (I_t^{3L} - e_t s_W^2) s_{\alpha+\beta} & -\frac{h_t}{\sqrt{2}}(A_t\, c_\alpha + \mu s_\alpha) \\ -\frac{h_t}{\sqrt{2}}(A_t\, c_\alpha + \mu s_\alpha) & -\sqrt{2}h_t m_t c_\alpha + g_Z m_Z e_t s_W^2 s_{\alpha+\beta} \end{pmatrix}, \\
G_{LR,1}^{\tilde{b}} &= \begin{pmatrix} \sqrt{2}h_b m_b s_\alpha + g_Z m_Z (I_b^{3L} - e_b s_W^2) s_{\alpha+\beta} & \frac{h_b}{\sqrt{2}}(A_b\, s_\alpha + \mu c_\alpha) \\ \frac{h_b}{\sqrt{2}}(A_b\, s_\alpha + \mu c_\alpha) & \sqrt{2}h_b m_b s_\alpha + g_Z m_Z e_b s_W^2 s_{\alpha+\beta} \end{pmatrix}, \\
G_{LR,2}^{\tilde{f}} &= G_{LR,1}^{\tilde{f}} \qquad \text{with } \alpha \to \alpha - \pi/2\,, \\
G_{LR,3}^{\tilde{t}} &= -\sqrt{2}h_t \begin{pmatrix} 0 & -\frac{i}{2}\Big(A_t\, c_\beta + \mu\, s_\beta\Big) \\ \frac{i}{2}\Big(A_t\, c_\beta + \mu\, s_\beta\Big) & 0 \end{pmatrix}, \\
G_{LR,3}^{\tilde{b}} &= -\sqrt{2}h_b \begin{pmatrix} 0 & -\frac{i}{2}\Big(A_b\, s_\beta + \mu\, c_\beta\Big) \\ \frac{i}{2}\Big(A_b\, s_\beta + \mu\, c_\beta\Big) & 0 \end{pmatrix}, \\
G_{LR,4}^{\tilde{f}} &= G_{LR,3}^{\tilde{f}} \qquad \text{with } \beta \to \beta - \pi/2\,,
\end{aligned}$$

where we have used the abbreviations $s_x \equiv \sin x$, $c_x \equiv \cos x$ and $s_W \equiv \sin\theta_W$. α denotes the mixing angle of the $\{h^0, H^0\}$–system, and h_t and h_b are the Yukawa couplings

$$h_t \;=\; \frac{g\, m_t}{\sqrt{2} m_W \sin\beta}\,, \qquad h_b \;=\; \frac{g\, m_b}{\sqrt{2} m_W \cos\beta}\,. \tag{31}$$

The couplings of charged Higgs bosons to two sfermions are given by ($l = 1, 2$)

$$G_{ijl}^{\tilde{f}\tilde{f}'} \;\equiv\; G\Big(H_l^{\pm} \tilde{f}_i^* \tilde{f}_j'\Big) \;=\; G_{jil}^{\tilde{f}'\tilde{f}} \;=\; \Big(R^{\tilde{f}}\, G_{LR,l}^{\tilde{f}\tilde{f}'} \Big(R^{\tilde{f}'}\Big)^T\Big)_{ij}\,, \tag{32}$$

$$G_{LR,1}^{\tilde{t}\tilde{b}} \;=\; \begin{pmatrix} h_b m_b \sin\beta + h_t m_t \cos\beta - \frac{g m_W}{\sqrt{2}} \sin 2\beta & h_b (A_b \sin\beta + \mu \cos\beta) \\ h_t (A_t \cos\beta + \mu \sin\beta) & h_t m_b \cos\beta + h_b m_t \sin\beta \end{pmatrix}, \tag{33}$$

$$G_{LR,1}^{\tilde{b}\tilde{t}} \;=\; \begin{pmatrix} h_b m_b \sin\beta + h_t m_t \cos\beta - \frac{g m_W}{\sqrt{2}} \sin 2\beta & h_t (A_t \cos\beta + \mu \sin\beta) \\ h_b (A_b \sin\beta + \mu \cos\beta) & h_t m_b \cos\beta + h_b m_t \sin\beta \end{pmatrix} \;=\; \Big(G_{LR,1}^{\tilde{t}\tilde{b}}\Big)^T\,, \tag{34}$$

$$G_{LR,2}^{\tilde{f}\tilde{f}'} \;=\; G_{LR,1}^{\tilde{f}\tilde{f}'} \qquad \text{with} \quad \beta \;\to\; \beta - \frac{\pi}{2}\,. \tag{35}$$

f' denotes the isospin partner of the fermion f, i. e. $t' = b$, $\tilde{b}'_i = \tilde{t}_i$ etc. Note that only the angle β explicitly given in the matrices above has to be substituted; the dependence of β in the Yukawa couplings has to remain the same.

The $H^0_k H^0_l \tilde{f}^*_i \tilde{f}_j$ interaction is given by

$$\mathcal{L} = -\frac{1}{2} \sum_f \Big[h_f^2 \, c_{kl}^{\tilde{f}} \, \delta_{ij} + g^2 \left(c_{kl}^{\tilde{b}} - c_{kl}^{\tilde{t}} \right) e_{ij}^{\tilde{f}} \Big] \, H^0_k H^0_l \, \tilde{f}^*_i \tilde{f}_j \,, \tag{36}$$

with

$$c_{kl}^{\tilde{b}} = \begin{pmatrix} \sin^2\alpha & -\frac{1}{2}\sin 2\alpha & 0 & 0 \\ -\frac{1}{2}\sin 2\alpha & \cos^2\alpha & 0 & 0 \\ 0 & 0 & \sin^2\beta & -\frac{1}{2}\sin 2\beta \\ 0 & 0 & -\frac{1}{2}\sin 2\beta & \cos^2\beta \end{pmatrix}, \tag{37}$$

$$c_{kl}^{\tilde{t}} = \begin{pmatrix} \cos^2\alpha & \frac{1}{2}\sin 2\alpha & 0 & 0 \\ \frac{1}{2}\sin 2\alpha & \sin^2\alpha & 0 & 0 \\ 0 & 0 & \cos^2\beta & \frac{1}{2}\sin 2\beta \\ 0 & 0 & \frac{1}{2}\sin 2\beta & \sin^2\beta \end{pmatrix}, \tag{38}$$

$$e_{ij}^{\tilde{f}} = \frac{1}{2c_W^2} \Big[(I_f^{3L} - e_f s_W^2) R_{i1}^{\tilde{f}} R_{j1}^{\tilde{f}} + e_f s_W^2 R_{i2}^{\tilde{f}} R_{j2}^{\tilde{f}} \Big] . \tag{39}$$

For the $H^+_k H^-_l \tilde{f}^*_i \tilde{f}_j$ interaction,

$$\mathcal{L} = -\frac{1}{2} \sum_f \Big[h_f^2 \, d_{kl}^{\tilde{f}} \Big(R_{i2}^{\tilde{f}} R_{j2}^{\tilde{f}} + R_{i1}^{\tilde{f}'} R_{j1}^{\tilde{f}'} \Big) + g^2 \left(d_{kl}^{\tilde{b}} - d_{kl}^{\tilde{t}} \right) f_{ij}^{\tilde{f}} \Big] \, H^+_k H^-_l \, \tilde{f}^*_i \tilde{f}_j \,, \tag{40}$$

we use the coupling matrices

$$d_{kl}^{\tilde{b}} = \begin{pmatrix} \sin^2\beta & -\frac{1}{2}\sin 2\beta & 0 & 0 \\ -\frac{1}{2}\sin 2\beta & \cos^2\beta & 0 & 0 \\ 0 & 0 & \sin^2\beta & -\frac{1}{2}\sin 2\beta \\ 0 & 0 & -\frac{1}{2}\sin 2\beta & \cos^2\beta \end{pmatrix}, \tag{41}$$

$$d_{kl}^{\tilde{t}} = \begin{pmatrix} \cos^2\beta & \frac{1}{2}\sin 2\beta & 0 & 0 \\ \frac{1}{2}\sin 2\beta & \sin^2\beta & 0 & 0 \\ 0 & 0 & \cos^2\beta & \frac{1}{2}\sin 2\beta \\ 0 & 0 & \frac{1}{2}\sin 2\beta & \sin^2\beta \end{pmatrix}, \tag{42}$$

$$f_{ij}^{\tilde{f}} = \frac{1}{2c_W^2} \Big[(- I_f^{3L} \cos 2\theta_W - e_f s_W^2) \, R_{i1}^{\tilde{f}} R_{j1}^{\tilde{f}} + e_f s_W^2 R_{i2}^{\tilde{f}} R_{j2}^{\tilde{f}} \Big] . \tag{43}$$

For the Higgs–fermion–fermion couplings the interaction Lagrangian reads

$$\mathcal{L} = \sum_{k=1}^{2} s_k^f \, H^0_k \bar{f} f + \sum_{k=3}^{4} s_k^f \, H^0_k \bar{f} \gamma^5 f + \sum_{l=1}^{2} \Big[H^+_l \bar{t} \, (y_l^b P_R + y_l^t P_L) \, b + \text{h.c.} \Big] \tag{44}$$

with the couplings

$$
\begin{aligned}
s_1^t &= -g\tfrac{m_t\cos\alpha}{2m_W\sin\beta} = -\tfrac{h_t}{\sqrt{2}}\cos\alpha, & s_1^b &= g\tfrac{m_b\sin\alpha}{2m_W\cos\beta} = \tfrac{h_b}{\sqrt{2}}\sin\alpha\,,\\
s_2^t &= -g\tfrac{m_t\sin\alpha}{2m_W\sin\beta} = -\tfrac{h_t}{\sqrt{2}}\sin\alpha, & s_2^b &= -g\tfrac{m_b\cos\alpha}{2m_W\cos\beta} = -\tfrac{h_b}{\sqrt{2}}\cos\alpha\,,\\
s_3^t &= ig\tfrac{m_t\cot\beta}{2m_W} = i\tfrac{h_t}{\sqrt{2}}\cos\beta, & s_3^b &= ig\tfrac{m_b\tan\beta}{2m_W} = i\tfrac{h_b}{\sqrt{2}}\sin\beta\,,\\
s_4^t &= ig\tfrac{m_t}{2m_W} = i\tfrac{h_t}{\sqrt{2}}\sin\beta, & s_4^b &= -ig\tfrac{m_b}{2m_W} = -i\tfrac{h_b}{\sqrt{2}}\cos\beta\,,\\
y_1^t &= g\tfrac{m_t\cot\beta}{\sqrt{2}m_W} = h_t\cos\beta, & y_1^b &= g\tfrac{m_b\tan\beta}{\sqrt{2}m_W} = h_b\sin\beta\,,\\
y_2^t &= g\tfrac{m_t}{\sqrt{2}m_W} = h_t\sin\beta, & y_2^b &= -g\tfrac{m_b}{\sqrt{2}m_W} = -h_b\cos\beta\,.
\end{aligned}
\tag{45}
$$

The interaction Lagrangian for Higgs bosons and gauginos is given by

$$
\begin{aligned}
\mathcal{L} &= -\frac{g}{2}\sum_{k=1}^{2} H_k^0\,\bar{\tilde{\chi}}_l^0 F_{lmk}^0\,\tilde{\chi}_m^0 - i\frac{g}{2}\sum_{k=3}^{4} H_k^0\,\bar{\tilde{\chi}}_l^0\,F_{lmk}^0\gamma_5\,\tilde{\chi}_m^0\\
&\quad -g\sum_{k=1}^{2} H_k^0\,\bar{\tilde{\chi}}_i^+\left(F_{ijk}^+P_R + F_{jik}^+P_L\right)\tilde{\chi}_j^+ + ig\sum_{k=3}^{4} H_k^0\,\bar{\tilde{\chi}}_i^+\left(F_{ijk}^+P_R + F_{jik}^+P_L\right)\tilde{\chi}_j^+\\
&\quad -g\sum_{k=1}^{2}\left[H_k^+\,\bar{\tilde{\chi}}_i^+\left(F_{ilk}^RP_R + F_{ilk}^LP_L\right)\tilde{\chi}_l^0 + \text{h.c.}\right].
\end{aligned}
\tag{46}
$$

with

$$
\begin{aligned}
F_{lmk}^0 &= \frac{e_k}{2}\left[Z_{l3}Z_{m2} + Z_{m3}Z_{l2} - \tan\theta_W\left(Z_{l3}Z_{m1} + Z_{m3}Z_{l1}\right)\right]\\
&\quad + \frac{d_k}{2}\left[Z_{l4}Z_{m2} + Z_{m4}Z_{l2} - \tan\theta_W\left(Z_{l4}Z_{m1} + Z_{m4}Z_{l1}\right)\right] = F_{mlk}^0\,,
\end{aligned}
\tag{47}
$$

$$
F_{ijk}^+ = \frac{1}{\sqrt{2}}\left(e_kV_{i1}U_{j2} - d_kV_{i2}U_{j1}\right)\,,
\tag{48}
$$

and

$$
\begin{aligned}
F_{ilk}^R &= d_{k+2}\left[V_{i1}Z_{l4} + \frac{1}{\sqrt{2}}(Z_{l2} + Z_{l1}\tan\theta_W)V_{i2}\right]\,,\\
F_{ilk}^L &= -e_{k+2}\left[U_{i1}Z_{l3} - \frac{1}{\sqrt{2}}(Z_{l2} + Z_{l1}\tan\theta_W)U_{i2}\right]\,.
\end{aligned}
\tag{49}
$$

U, V and Z are rotation matrices which diagonalize the chargino and neutralino mass matrices. d_k and e_k take the values

$$
d_k = \{-\cos\alpha, -\sin\alpha, \cos\beta, \sin\beta\}\,, \qquad e_k = \{-\sin\alpha, \cos\alpha, -\sin\beta, \cos\beta\}\,.
$$

The coupling of the vector boson Z^0 to two sfermions, $\mathcal{L} = -i\, g_Z\, z_{ij}^{\tilde{f}}\, Z_\mu^0\, \tilde{f}_i^*\, \overleftrightarrow{\partial^\mu}\, \tilde{f}_j$ with $g_Z = g/\cos\theta_W$, is given by the matrix

$$z_{ij}^{\tilde{f}} \;=\; C_L^f\, R_{i1}^{\tilde{f}} R_{j1}^{\tilde{f}} + C_R^f\, R_{i2}^{\tilde{f}} R_{j2}^{\tilde{f}}$$

with $C_L^f = I_f^{3L} - e_f s_W^2$ and $C_R^f = -e_f s_W^2$.
For the interaction of a vector boson with two gauginos we use the couplings

$$O_{ij}^L \;=\; Z_{i2}V_{j1} - \tfrac{1}{\sqrt{2}} Z_{i4} V_{j2}\,, \qquad O_{ij}^R \;=\; Z_{i2}U_{j1} + \tfrac{1}{\sqrt{2}} Z_{i3} U_{j2}\,,$$

$$\begin{aligned} O_{ij}^{\prime L} &= -V_{i1}V_{j1} - \tfrac{1}{2} V_{i2}V_{j2} + \delta_{ij} s_W^2\,, \\ O_{ij}^{\prime R} &= -U_{i1}U_{j1} - \tfrac{1}{2} U_{i2}U_{j2} + \delta_{ij} s_W^2\,, \\ O_{ij}^{\prime\prime L} &= -\tfrac{1}{2} Z_{i3}Z_{j3} + \tfrac{1}{2} Z_{i4}Z_{j4} \;=\; -O_{ij}^{\prime\prime R}\,. \end{aligned}$$

The interaction Lagrangian of the chargino–sfermion–fermion couplings is given by

$$\begin{aligned} \mathcal{L} \;=\;& \bar{t}\left(l_{ij}^{\tilde{b}} P_R + k_{ij}^{\tilde{b}} P_L\right) \tilde{\chi}_j^+ \tilde{b}_i + \bar{b}\left(l_{ij}^{\tilde{t}} P_R + k_{ij}^{\tilde{t}} P_L\right) \tilde{\chi}_j^{+c}\, \tilde{t}_i \\ &+ \overline{\tilde{\chi}_j^+}\left(l_{ij}^{\tilde{b}} P_L + k_{ij}^{\tilde{b}} P_R\right) t\, \tilde{b}_i^* + \overline{\tilde{\chi}_j^{+c}}\left(l_{ij}^{\tilde{t}} P_L + k_{ij}^{\tilde{t}} P_R\right) b\, \tilde{t}_i^* \end{aligned} \tag{50}$$

with the coupling matrices

$$\begin{aligned} l_{ij}^{\tilde{t}} &= -gV_{j1}R_{i1}^{\tilde{t}} + h_t V_{j2} R_{i2}^{\tilde{t}}\,, & l_{ij}^{\tilde{b}} &= -gU_{j1}R_{i1}^{\tilde{b}} + h_b U_{j2} R_{i2}^{\tilde{b}}\,, \\ k_{ij}^{\tilde{t}} &= h_b U_{j2} R_{i1}^{\tilde{t}}\,, & k_{ij}^{\tilde{b}} &= h_t V_{j2} R_{i1}^{\tilde{b}}\,. \end{aligned} \tag{51}$$

For the neutralino–sfermion–fermion couplings the Lagrangian reads

$$\mathcal{L} \;=\; \bar{f}\left(a_{ik}^{\tilde{f}} P_R + b_{ik}^{\tilde{f}} P_L\right) \tilde{\chi}_k^0\, \tilde{f}_i + \bar{\tilde{\chi}}_k^0 \left(a_{ik}^{\tilde{f}} P_L + b_{ik}^{\tilde{f}} P_R\right) f\, \tilde{f}_i^* \tag{52}$$

with the coupling matrices

$$a_{ik}^{\tilde{f}} \;=\; h_f Z_{kx} R_{i2}^{\tilde{f}} + g f_{Lk}^f R_{i1}^{\tilde{f}}\,, \qquad b_{ik}^{\tilde{f}} \;=\; h_f Z_{kx} R_{i1}^{\tilde{f}} + g f_{Rk}^f R_{i2}^{\tilde{f}} \tag{53}$$

and

$$f_{Lk}^f = \sqrt{2}\left((e_f - I_f^{3L})\tan\theta_W Z_{k1} + I_f^{3L} Z_{k2}\right)\,, \quad f_{Rk}^f = -\sqrt{2} e_f \tan\theta_W Z_{k1}\,. \tag{54}$$

x takes the values $\{3, 4\}$ for {down, up}–type case, respectively.

B Vertex corrections

Here we give the explicit form of the electroweak contributions to the vertex corrections which are depicted in Fig. 12. For SUSY–QCD contributions we refer to [8].

$$\begin{aligned} \delta G_{123}^{\tilde{f}(v)} \;=\;& \delta G_{123}^{\tilde{f}(v,H\tilde{f}\tilde{f})} + \delta G_{123}^{\tilde{f}(v,\tilde{f}HH)} + \delta G_{123}^{\tilde{f}(v,\tilde{\chi}ff)} + \delta G_{123}^{\tilde{f}(v,f\tilde{\chi}\tilde{\chi})} \\ &+ \delta G_{123}^{\tilde{f}(v,V)} + \delta G_{123}^{\tilde{f}(v,\tilde{f}\tilde{f})} + \delta G_{123}^{\tilde{f}(v,H\tilde{f})} + \delta G_{123}^{\tilde{f}(v,AZ)} + \delta G_{123}^{\tilde{f}(v,AG)} \end{aligned} \tag{55}$$

The single contributions correspond to the diagrams with three scalar particles $\left(\delta G_{123}^{\tilde{f}(v,H\tilde{f}\tilde{f})}\right.$ and $\left.\delta G_{123}^{\tilde{f}(v,HH\tilde{f})}\right)$, three fermions $\left(\delta G_{123}^{\tilde{f}(v,\tilde{\chi}ff)}\right.$ and $\left.\delta G_{123}^{\tilde{f}(v,f\tilde{\chi}\tilde{\chi})}\right)$, one vector particle $\left(\delta G_{123}^{\tilde{f}(v,V)}\right)$ or two scalar particles $\left(\delta G_{123}^{\tilde{f}(v,\tilde{f}\tilde{f})}\right.$ and $\left.\delta G_{123}^{\tilde{f}(v,H\tilde{f})}\right)$ in the loop. $\delta G_{123}^{\tilde{f}(v,AZ\mathrm{mix})}$ denotes the correction due to the mixing of A^0 and Z^0 and $\delta G_{123}^{\tilde{f}(v,AG)}$ is the Higgs mixing transition A^0–G^0.

As shown in [12] we can sum up the A^0Z^0 and A^0G^0 transition amplitudes which leads to

$$\delta G_{123}^{\tilde{f}(v,AZ)} + \delta G_{123}^{\tilde{f}(v,AG)} \;=\; -\frac{i}{m_Z}\,\Pi_{AZ}(m^2_{A^0})\,G^{\tilde{f}}_{124}\,. \tag{56}$$

The explicit form of the A^0–Z^0 self–energy, $\Pi_{AZ}(m^2_{A^0})$, is given in app. D.1. The vertex corrections from the exchange of one Higgs and two sfermions are

$$\begin{aligned}
\delta G_{123}^{\tilde{f}(v,H\tilde{f}\tilde{f})} \;=\; & -\frac{1}{(4\pi)^2}\sum_{m,n=1}^{2}\sum_{k=1}^{4} G^{\tilde{f}}_{mn3}G^{\tilde{f}}_{imk}G^{\tilde{f}}_{njk}\,C_0\Big(m^2_{\tilde{f}_i},m^2_{A^0},m^2_{\tilde{f}_j},m^2_{H^0_k},m^2_{\tilde{f}_m},m^2_{\tilde{f}_n}\Big) \\
& -\frac{1}{(4\pi)^2}\sum_{m,n=1}^{2}\sum_{k=1}^{2} G^{\tilde{f}'}_{mn3}G^{\tilde{f}\tilde{f}'}_{imk}G^{\tilde{f}\tilde{f}'}_{jnk}\,C_0\Big(m^2_{\tilde{f}_i},m^2_{A^0},m^2_{\tilde{f}_j},m^2_{H^+_k},m^2_{\tilde{f}'_m},m^2_{\tilde{f}'_n}\Big)
\end{aligned} \tag{57}$$

with the standard two–point function C_0 [23] for which we follow the conventions of [24]. The graph with 2 Higgs particles and one sfermion in the loop leads to

$$\begin{aligned}
\delta G_{123}^{\tilde{f}(v,\tilde{f}HH)} \;=\; & -\frac{1}{(4\pi)^2}\frac{g_Z\,m_Z}{2}\sum_{m=1}^{2}\left(\sum_{k=1}^{2}\sum_{l=3}^{4} G^{\tilde{f}}_{imk}G^{\tilde{f}}_{mjl}\,A_{k,l-2} + \sum_{k=3}^{4}\sum_{l=1}^{2} G^{\tilde{f}}_{imk}G^{\tilde{f}}_{mjl}\,A_{l,k-2}\right)\times \\
& \qquad C_0\Big(m^2_{\tilde{f}_i},m^2_{A^0},m^2_{\tilde{f}_j},m^2_{\tilde{f}_m},m^2_{H^0_k},m^2_{H^0_l}\Big) \\
& -\frac{i}{(4\pi)^2}\,I_f^{3L}\,g\,m_W\sum_{m=1}^{2}\Big(G^{\tilde{f}\tilde{f}'}_{im1}G^{\tilde{f}\tilde{f}'}_{jm2}\,C_0\Big(m^2_{\tilde{f}_i},m^2_{A^0},m^2_{\tilde{f}_j},m^2_{\tilde{f}'_m},m^2_{H^+},m^2_{G^+}\Big) \\
& \qquad -G^{\tilde{f}\tilde{f}'}_{im2}\,G^{\tilde{f}\tilde{f}'}_{jm1}\,C_0\Big(m^2_{\tilde{f}_i},m^2_{A^0},m^2_{\tilde{f}_j},m^2_{\tilde{f}'_m},m^2_{G^+},m^2_{H^+}\Big)\Big)
\end{aligned}$$

with

$$A_{kl} \;=\; \begin{pmatrix} -\cos 2\beta\,\sin(\alpha+\beta) & -\sin 2\beta\,\sin(\alpha+\beta) \\ \cos 2\beta\,\cos(\alpha+\beta) & \sin 2\beta\,\cos(\alpha+\beta) \end{pmatrix}.$$

For the gaugino exchange contributions we get

$$\begin{aligned}
\delta G_{123}^{\tilde{f}(v,\tilde{\chi}ff)} \;=\; & \frac{1}{(4\pi)^2}\sum_{k=1}^{4} F\Big(m^2_{\tilde{f}_i},m^2_{A^0},m^2_{\tilde{f}_j},m_{\tilde{\chi}^0_k},m_f,m_f;s^f_3,-s^f_3,b^{\tilde{f}}_{ik},a^{\tilde{f}}_{ik},a^{\tilde{f}}_{jk},b^{\tilde{f}}_{jk}\Big) \\
& +\frac{1}{(4\pi)^2}\sum_{k=1}^{2} F\Big(m^2_{\tilde{f}_i},m^2_{A^0},m^2_{\tilde{f}_j},m_{\tilde{\chi}^+_k},m_{f'},m_{f'};s^{f'}_3,-s^{f'}_3,k^{\tilde{f}}_{ik},l^{\tilde{f}}_{ik},l^{\tilde{f}}_{jk},k^{\tilde{f}}_{jk}\Big)\,,
\end{aligned}$$

$$\delta G_{123}^{\tilde{f}(v,f\tilde{\chi}\tilde{\chi})} = \frac{1}{(4\pi)^2}\sum_{k,l=1}^{4} F\Big(m^2_{\tilde{f}_i}, m^2_{A^0}, m^2_{\tilde{f}_j}, m_f, m_{\tilde{\chi}^0_k}, m_{\tilde{\chi}^0_l}; igF^0_{lk3}, -igF^0_{lk3}, b^{\tilde{f}}_{ik}, a^{\tilde{f}}_{ik}, a^{\tilde{f}}_{jl}, b^{\tilde{f}}_{jl}\Big)$$
$$+\frac{1}{(4\pi)^2}\sum_{k,l=1}^{2} F\Big(m^2_{\tilde{f}_i}, m^2_{A^0}, m^2_{\tilde{f}_j}, m_{f'}, m_{\tilde{\chi}^+_k}, m_{\tilde{\chi}^+_l}; ig\widetilde{F}^+_{kl3}, -ig\widetilde{F}^+_{lk3}, k^{\tilde{f}}_{ik}, l^{\tilde{f}}_{ik}, l^{\tilde{f}}_{jl}, k^{\tilde{f}}_{jl}\Big)\,, \tag{58}$$

where $F(\ldots)$ shortly stands for

$$\begin{aligned} F\Big(m_1^2, m_0^2, m_2^2, M_0, M_1, M_2; g_0^R, g_0^L, g_1^R, g_1^L, g_2^R, g_2^L\Big) &= (h_1M_1+h_2M_2)B_0(m_0^2, M_1^2, M_2^2) \\ &+ (h_0M_0+h_1M_1)B_0(m_1^2, M_0^2, M_1^2) + (h_0M_0+h_2M_2)B_0(m_2^2, M_0^2, M_2^2) \\ &+ \Big[2\Big(g_0^Rg_1^Rg_2^R+g_0^Lg_1^Lg_2^L\Big)M_0M_1M_2 + h_0M_0\Big(M_1^2+M_2^2-m_0^2\Big) + h_1M_1\Big(M_0^2+M_2^2-m_2^2\Big) \\ &+ h_2M_2\Big(M_0^2+M_1^2-m_1^2\Big)\Big]C_0(m_1^2, m_0^2, m_2^2, M_0^2, M_1^2, M_2^2) \end{aligned} \tag{59}$$

with the abbreviations $h_0 = \Big(g_0^Lg_1^Rg_2^R + g_0^Rg_1^Lg_2^L\Big), h_1 = \Big(g_0^Lg_1^Lg_2^R + g_0^Rg_1^Rg_2^L\Big)$ and $h_2 = \Big(g_0^Rg_1^Lg_2^R + g_0^Lg_1^Rg_2^L\Big)$. For up–type sfermions $\widetilde{F}^+_{kl3} = F^+_{kl3}$ and for down–type sfermions chargino indices are interchanged, $\widetilde{F}^+_{kl3} = F^+_{lk3}$.
We split the irreducible vertex graphs with one vector particle in the loop into the single contributions of the photon, the Z–boson and the W–boson,

$$\delta G_{123}^{\tilde{f}(v,V)} = \delta G_{123}^{\tilde{f}(v,\gamma)} + \delta G_{123}^{\tilde{f}(v,Z)} + \delta G_{123}^{\tilde{f}(v,W)}\,. \tag{60}$$

In order to regularize the infrared divergences we introduce a photon mass λ. Thus we have

$$\begin{aligned} \delta G_{123}^{\tilde{f}(v,\gamma)} &= \frac{1}{(4\pi)^2}(e_0e_f)^2 G^{\tilde{f}}_{123}\; V\Big(m^2_{\tilde{f}_i}, m^2_{A^0}, m^2_{\tilde{f}_j}, \lambda^2, m^2_{\tilde{f}_i}, m^2_{\tilde{f}_j}\Big)\,, \\ \delta G_{123}^{\tilde{f}(v,Z)} &= \frac{1}{(4\pi)^2} g_Z^2 \sum_{m,n=1}^{2} G^{\tilde{f}}_{mn3}\, z^{\tilde{f}}_{im}\, z^{\tilde{f}}_{nj}\; V\Big(m^2_{\tilde{f}_i}, m^2_{A^0}, m^2_{\tilde{f}_j}, m^2_Z, m^2_{\tilde{f}_m}, m^2_{\tilde{f}_n}\Big) \\ &\quad -\frac{i}{(4\pi)^2}\frac{g_Z^2}{2}\sum_{k,m=1}^{2} G^{\tilde{f}}_{mjk}\, z^{\tilde{f}}_{im}\, R_{1k}(\alpha-\beta)\; V\Big(m^2_{A^0}, m^2_{\tilde{f}_j}, m^2_{\tilde{f}_i}, m^2_Z, m^2_{H^0_k}, m^2_{\tilde{f}_m}\Big) \\ &\quad +\frac{i}{(4\pi)^2}\frac{g_Z^2}{2}\sum_{k,m=1}^{2} G^{\tilde{f}}_{imk}\, z^{\tilde{f}}_{mj}\, R_{1k}(\alpha-\beta)\; V\Big(m^2_{\tilde{f}_j}, m^2_{\tilde{f}_i}, m^2_{A^0}, m^2_Z, m^2_{\tilde{f}_m}, m^2_{H^0_k}\Big)\,, \\ \delta G_{123}^{\tilde{f}(v,W)} &= \frac{1}{(4\pi)^2}\frac{g^2}{2}\sum_{m,n=1}^{2} G^{\tilde{f}'}_{mn3}\, R^{\tilde{f}}_{i1}R^{\tilde{f}}_{j1}R^{\tilde{f}'}_{m1}R^{\tilde{f}'}_{n1}\; V\Big(m^2_{\tilde{f}_i}, m^2_{A^0}, m^2_{\tilde{f}_j}, m^2_W, m^2_{\tilde{f}'_m}, m^2_{\tilde{f}'_n}\Big) \\ &\quad +\frac{i}{(4\pi)^2}\frac{g^2}{2\sqrt{2}}\sum_{m=1}^{2} G^{\tilde{f}\tilde{f}'}_{jm1}\, R^{\tilde{f}}_{i1}R^{\tilde{f}'}_{m1}\; V\Big(m^2_{A^0}, m^2_{\tilde{f}_j}, m^2_{\tilde{f}_i}, m^2_W, m^2_{H^+}, m^2_{\tilde{f}'_m}\Big) \\ &\quad -\frac{i}{(4\pi)^2}\frac{g^2}{2\sqrt{2}}\sum_{m=1}^{2} G^{\tilde{f}\tilde{f}'}_{im1}\, R^{\tilde{f}'}_{m1}R^{\tilde{f}}_{j1} V\Big(m^2_{\tilde{f}_j}, m^2_{\tilde{f}_i}, m^2_{A^0}, m^2_W, m^2_{\tilde{f}'_m}, m^2_{H^+}\Big)\,, \end{aligned} \tag{61}$$

where we have used the vector vertex function

$$V\Big(m_1^2,m_0^2,m_2^2,M_0^2,M_1^2,M_2^2\Big) \;=\; -B_0\Big(m_0^2,M_1^2,M_2^2\Big)+B_0\Big(m_1^2,M_0^2,M_1^2\Big)+B_0\Big(m_2^2,M_0^2,M_2^2\Big)$$
$$+\;\Big(-2m_0^2+m_1^2+m_2^2-M_0^2+M_1^2+M_2^2\Big)\,C_0\Big(m_1^2,m_0^2,m_2^2,M_0^2,M_1^2,M_2^2\Big) \qquad (62)$$

and the rotation matrix R_{kl},

$$R_{kl}(\phi) \;\equiv\; \left(\begin{array}{cc} \cos\phi & \sin\phi \\ -\sin\phi & \cos\phi \end{array}\right)_{kl} .$$

$z_{ij}^{\tilde f}$ can be found in Appendix A.
For the vertex graphs with 2 sfermions in the loop we obtain

$$\begin{aligned}
\delta G_{123}^{\tilde f(v,\tilde f\tilde f)} \;=\; & -\frac{1}{(4\pi)^2}\,h_f^2\sum_{m,n=1}^{2} G_{nm3}^{\tilde f}\Big[R_{ijmn}^{\tilde f}+R_{mnij}^{\tilde f}+N_C^f\Big(R_{inmj}^{\tilde f}+R_{mjin}^{\tilde f}\Big)\Big]B_0\Big(m_{A^0}^2,m_{\tilde f_m}^2,m_{\tilde f_n}^2\Big) \\
& -\frac{1}{(4\pi)^2}\,g_Z^2\sum_{m,n=1}^{2} G_{nm3}^{\tilde f}\Big\{\Big[\Big(\frac14-(2I_f^{3L}-e_f)e_f s_W^2\Big)R_{ijmn}^{\tilde f_L}+e_f^2 s_W^2 R_{ijmn}^{\tilde f_R}\Big](N_C^f+1) \\
& \qquad +(I_f^{3L}-e_f)e_f s_W^2\Big[N_C^f\Big(R_{ijmn}^{\tilde f}+R_{mnij}^{\tilde f}\Big)+R_{inmj}^{\tilde f}+R_{mjin}^{\tilde f}\Big]\Big\} \\
& \qquad \times B_0\Big(m_{A^0}^2,m_{\tilde f_m}^2,m_{\tilde f_n}^2\Big) \\
& -\frac{1}{(4\pi)^2}\,N_C^{\hat f}\,h_f h_{\hat f}\sum_{m,n=1}^{2} G_{nm3}^{\hat{\tilde f}}\Big(R_{ijnm}^{\tilde f\hat{\tilde f}_F}+R_{jimn}^{\tilde f\hat{\tilde f}_F}\Big)B_0\Big(m_{A^0}^2,m_{\hat{\tilde f}_m}^2,m_{\hat{\tilde f}_n}^2\Big)\,. \qquad (63)
\end{aligned}$$

For various products of sfermion rotation matrices we have introduced the short forms

$$\begin{aligned}
R_{ijkl}^{\tilde f_L} \;&=\; R_{i1}^{\tilde f}R_{j1}^{\tilde f}R_{k1}^{\tilde f}R_{l1}^{\tilde f}\,, & R_{ijkl}^{\tilde f} \;&=\; R_{i1}^{\tilde f}R_{j1}^{\tilde f}R_{k2}^{\tilde f}R_{l2}^{\tilde f}\,, \\
R_{ijkl}^{\tilde f_R} \;&=\; R_{i2}^{\tilde f}R_{j2}^{\tilde f}R_{k2}^{\tilde f}R_{l2}^{\tilde f}\,, & R_{ijkl}^{\tilde f\hat{\tilde f}_F} \;&=\; R_{i1}^{\tilde f}R_{j2}^{\tilde f}R_{k1}^{\hat{\tilde f}}R_{l2}^{\hat{\tilde f}}\,.
\end{aligned} \qquad (64)$$

Note that the last term in eq. (63) originates from the mixing of 2 squarks and 2 sleptons, where $\hat f$ denotes the 'family partner' of the fermion f with the same isospin and from the same generation, i.e. $\hat t=\nu_\tau$ or $\hat{\tilde\tau}_i=\tilde b_i$. The diagrams with one Higgs boson and one sfermion in the loop lead to

$$\begin{aligned}
\delta G_{123}^{\tilde f(v,H\tilde f)} \;=\; & -\frac{1}{(4\pi)^2}\sum_{k=3}^{4}\sum_{m=1}^{2} G_{imk}^{\tilde f}\Big(h_f^2\,c_{3k}^{\tilde f}\,\delta_{mj}+g^2\Big(c_{3k}^{\tilde b}-c_{3k}^{\tilde t}\Big)e_{mj}^{\tilde f}\Big)B_0\Big(m_{A^0}^2,m_{H_k^0}^2,m_{\tilde f_m}^2\Big) \\
& +\frac{i}{(4\pi)^2}\,\sqrt2\,I_f^{3L}\sum_{k,m=1}^{2} G_{imk}^{\tilde f\tilde f'}\Bigg[\left\{\begin{array}{l}(h_\uparrow^2-g^2/2)\cos^2\beta-(h_\downarrow^2-g^2/2)\sin^2\beta \\ (h_f^2+h_{f'}^2-g^2)\sin\beta\cos\beta\end{array}\right\}_k R_{m1}^{\tilde f'}R_{j1}^{\tilde f} \\
& \qquad +h_f h_{f'}\,\delta_{k2}\,R_{m2}^{\tilde f'}R_{j2}^{\tilde f}\Bigg]B_0\Big(m_{A^0}^2,m_{H_k^+}^2,m_{\tilde f'_m}^2\Big) \\
& -\,i\leftrightarrow j\,.
\end{aligned}$$

with $h_\uparrow=\{h_t,0\}$ and $h_\downarrow=\{h_b,h_\tau\}$ for the decay into {squarks, sleptons}, respectively. The Higgs–Sfermion coupling matrices $c_{kl}^{\tilde f}$ and $e_{ij}^{\tilde f}$ can be found in Appendix A.

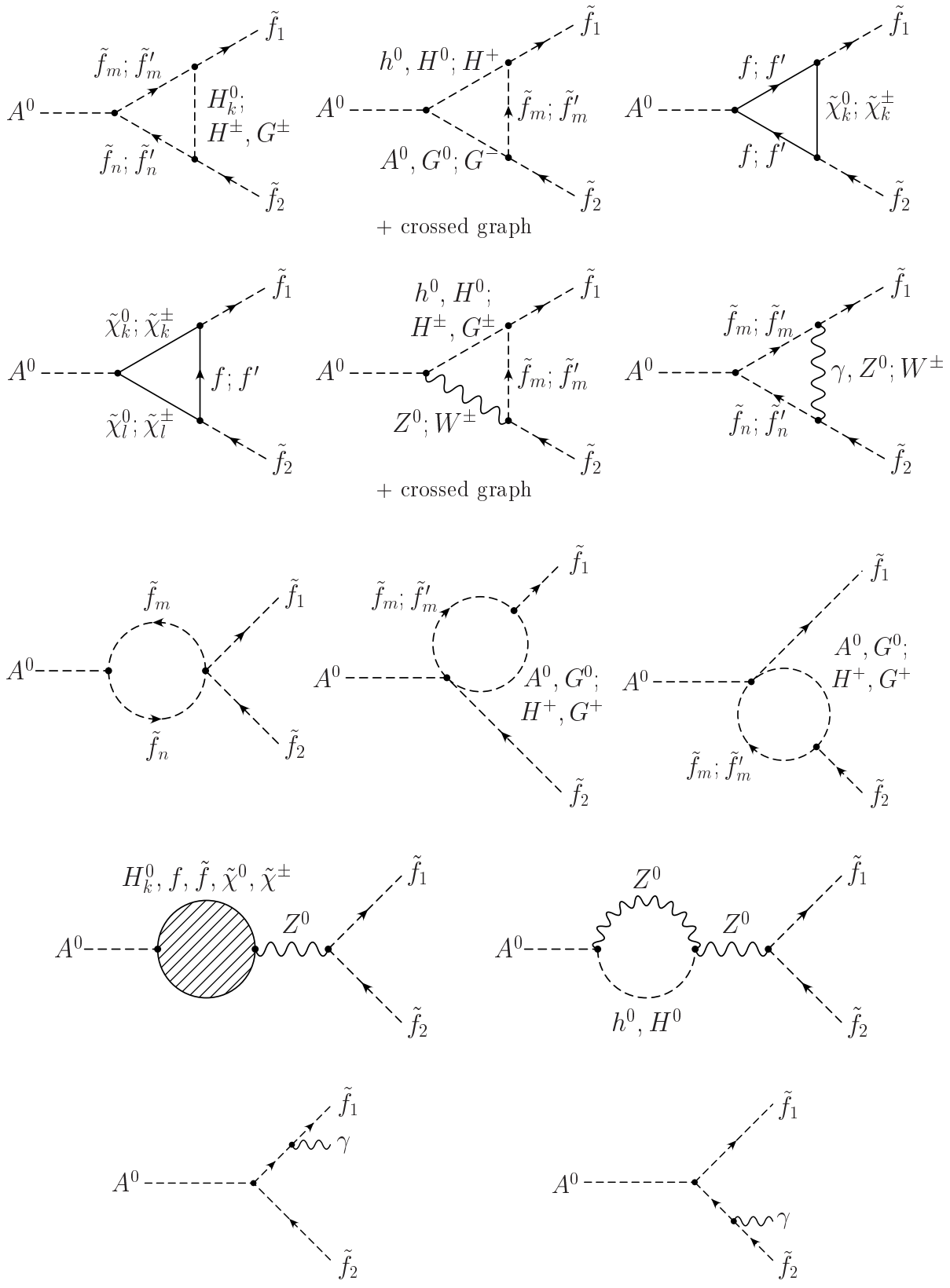

Figure 12: Vertex and photon emission diagrams relevant to the calculation of the virtual electroweak corrections to the decay width $A^0 \to \tilde{f}_1\bar{\tilde{f}}_2$.

C Diagonal Wave–function corrections

For the diagonal wave–function renormalization constants we use the conventional on–shell renormalization conditions which lead to

$$\delta Z_{33}^H \;=\; -\,\Re\,\dot{\Pi}_{33}^H(m^2_{A^0})\,, \qquad \delta Z_{ii}^{\tilde{f}} \;=\; -\,\Re\,\dot{\Pi}_{ii}^{\tilde{f}}(m^2_{\tilde{f}_i})\,, \tag{65}$$

where the dot in $\dot{\Pi}_{ii}(k^2)$ denotes the derivative with respect to k^2. In the following we list the single contributions of the wave–function corrections (Fig. 13 and 14).

C.1 Higgs part

$$\delta Z_{33}^{H,f} \;=\; \frac{2}{(4\pi)^2}\sum_f N_C^f \left(s_3^f\right)^2 \Big[B_0(m^2_{A^0},m_f^2,m_f^2) + m^2_{A^0}\dot{B}_0(m^2_{A^0},m_f^2,m_f^2)\Big] \tag{66}$$

$$\delta Z_{33}^{H,\tilde{f}} \;=\; -\frac{1}{(4\pi)^2}\sum_f \sum_{m,n=1}^{2} N_C^f\, G^{\tilde{f}}_{mn3}\, G^{\tilde{f}}_{nm3}\, \dot{B}_0(m^2_{A^0},m^2_{\tilde{f}_m},m^2_{\tilde{f}_n}) \tag{67}$$

$$\begin{aligned}\delta Z_{33}^{H,\tilde{\chi}^0} \;=\; \frac{1}{(4\pi)^2}\, g^2 \sum_{k,l=1}^{4} (F^0_{kl3})^2 \Big[&\dot{B}_0(m^2_{A^0},m^2_{\tilde{\chi}^0_k},m^2_{\tilde{\chi}^0_l})\Big((m_{\tilde{\chi}^0_k}-m_{\tilde{\chi}^0_l})^2 - m^2_{A^0}\Big) \\ &- B_0(m^2_{A^0},m^2_{\tilde{\chi}^0_k},m^2_{\tilde{\chi}^0_l})\Big]\end{aligned} \tag{68}$$

$$\begin{aligned}\delta Z_{33}^{H,\tilde{\chi}^+} \;=\; \frac{1}{(4\pi)^2}\, g^2 \sum_{k,l=1}^{2} \Big[&\Big((F^+_{kl3})^2 + (F^+_{lk3})^2\Big)\Big(\Big(m^2_{\tilde{\chi}^+_k} + m^2_{\tilde{\chi}^+_l} - m^2_{A^0}\Big)\dot{B}_0 - B_0\Big) \\ &- 4 m_{\tilde{\chi}^+_k} m_{\tilde{\chi}^+_l} F^+_{kl3}\, F^+_{lk3}\, \dot{B}_0\Big](m^2_{A^0},m^2_{\tilde{\chi}^+_k},m^2_{\tilde{\chi}^+_l})\end{aligned} \tag{69}$$

$$\begin{aligned}\delta Z_{33}^{H,H} \;=\; &-\frac{1}{(4\pi)^2}\Big(\frac{g_Z\, m_Z}{2}\Big)^2 \sum_{k=1}^{2}\sum_{l=3}^{4}\Big(A_{k,l-2}\Big)^2\, \dot{B}_0(m^2_{A^0},m^2_{H^0_k},m^2_{H^0_l}) \\ &- \frac{1}{(4\pi)^2}\, 2\,\Big(\frac{g\, m_W}{2}\Big)^2\, \dot{B}_0(m^2_{A^0},m^2_{H^+},m^2_{W^+})\end{aligned} \tag{70}$$

$$\begin{aligned}\delta Z_{33}^{H,Z} \;=\; \frac{1}{(4\pi)^2}\,\frac{g_Z^2}{4}\sum_{k=1}^{2}\Big(R_{1k}(\alpha-\beta)\Big)^2 \Big[&\dot{B}_0(m^2_{A^0},m^2_{H^0_k},m^2_Z)\Big(2m^2_{A^0}+2m^2_{H^0_k}-m^2_Z\Big) \\ &+ 2B_0(m^2_{A^0},m^2_{H^0_k},m^2_Z)\Big]\end{aligned} \tag{71}$$

$$\begin{aligned}\delta Z_{33}^{H,W} \;=\; \frac{1}{(4\pi)^2}\, 2\,\frac{g^2}{4}\Big[&\dot{B}_0(m^2_{A^0},m^2_{H^+},m^2_W)\Big(2m^2_{A^0}+2m^2_{H^+}-m^2_W\Big) \\ &+ 2B_0(m^2_{A^0},m^2_{H^+},m^2_W)\Big]\end{aligned} \tag{72}$$

C.2 Sfermion part

$$\delta Z_{ii}^{\tilde{f},\tilde{\chi}} = \frac{1}{(4\pi)^2}\sum_{k=1}^{4}\Big[\Big((a_{ik}^{\tilde{f}})^2+(b_{ik}^{\tilde{f}})^2\Big)\cdot\Big((m^2_{\tilde{\chi}_k^0}+m_f^2-m^2_{\tilde{f}_i})\,\dot{B}_0-B_0\Big) +4m_{\tilde{\chi}_k^0}m_f\,a_{ik}^{\tilde{f}}b_{ik}^{\tilde{f}}\,\dot{B}_0\Big](m^2_{\tilde{f}_i},m^2_{\tilde{\chi}_k^0},m_f^2)$$

$$+\frac{1}{(4\pi)^2}\sum_{k=1}^{2}\Big[\Big((k_{ik}^{\tilde{f}})^2+(l_{ik}^{\tilde{f}})^2\Big)\cdot\Big((m^2_{\tilde{\chi}_k^+}+m_{f'}^2-m^2_{\tilde{f}_i})\,\dot{B}_0-B_0\Big) +4m_{\tilde{\chi}_k^+}m_{f'}\,k_{ik}^{\tilde{f}}l_{ik}^{\tilde{f}}\,\dot{B}_0\Big](m^2_{\tilde{f}_i},m^2_{\tilde{\chi}_k^+},m^2_{f'}) \tag{73}$$

$$\delta Z_{ii}^{\tilde{f},H} = -\frac{1}{(4\pi)^2}\sum_{k=1}^{4}\sum_{m=1}^{2}G^{\tilde{f}}_{mik}\,G^{\tilde{f}}_{imk}\,\dot{B}_0(m^2_{\tilde{f}_i},m^2_{\tilde{f}_m},m^2_{H_k^0})$$

$$-\frac{1}{(4\pi)^2}\sum_{k=1}^{2}\sum_{m=1}^{2}G^{\tilde{f}'\tilde{f}}_{mik}\,G^{\tilde{f}\tilde{f}'}_{imk}\,\dot{B}_0(m^2_{\tilde{f}_i},m^2_{\tilde{f}'_m},m^2_{H_k^+}) \tag{74}$$

$$\delta Z_{ii}^{\tilde{f},\gamma} = \frac{1}{(4\pi)^2}\,(e_0e_f)^2\Big[2B_0+\Big(4m^2_{\tilde{f}_i}-\lambda^2\Big)\dot{B}_0\Big](m^2_{\tilde{f}_i},m^2_{\tilde{f}_i},\lambda^2)$$

$$\delta Z_{ii}^{\tilde{f},Z} = \frac{1}{(4\pi)^2}\,g_Z^2\sum_{m=1}^{2}\Big(z_{im}^{\tilde{f}}\Big)^2\Big[2B_0+\Big(2m^2_{\tilde{f}_i}+2m^2_{\tilde{f}_m}-m_Z^2\Big)\dot{B}_0\Big](m^2_{\tilde{f}_i},m^2_{\tilde{f}_m},m_Z^2) \tag{75}$$

$$\delta Z_{ii}^{\tilde{f},W} = \frac{1}{(4\pi)^2}\,\frac{g^2}{2}\sum_{m=1}^{2}\Big(R_{i1}^{\tilde{f}}R_{m1}^{\tilde{f}'}\Big)^2\Big[2B_0+\Big(2m^2_{\tilde{f}_i}+2m^2_{\tilde{f}'_m}-m_W^2\Big)\dot{B}_0\Big](m^2_{\tilde{f}_i},m^2_{\tilde{f}'_m},m_W^2) \tag{76}$$

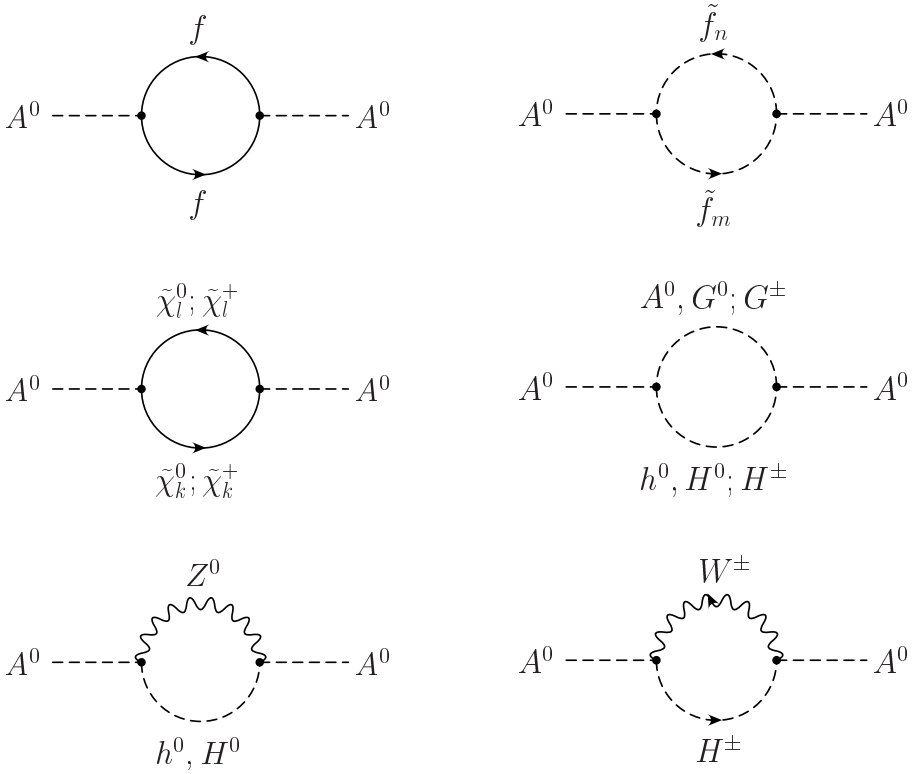

Figure 13: Diagonal Higgs self–energies

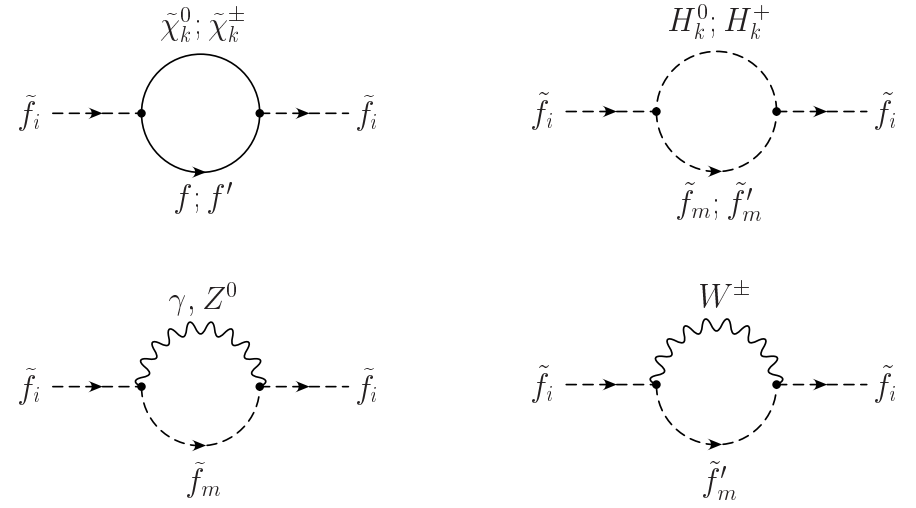

Figure 14: Diagonal sfermion self–energies

D Self–energies and counter terms

Here we give the explicit form of the self–energies needed for the computation of various counter terms for the one–loop width $A^0 \to \tilde{f}_1 \bar{\tilde{f}}_2$.

D.1 AZ–mixing

The scalar–vector mixing self–energy, $\Pi_{AZ}(k^2)$, is defined by the two–point function

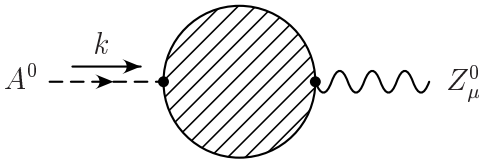

$$\mathcal{M} = -i\, k^\mu\, \Pi_{AZ}(k^2)\, \epsilon^*_\mu(k)\,.$$

The single contributions from the particles x are denoted by the superscript x in Π^x_{AZ}.

$$\Pi^f_{AZ} = -\frac{i}{(4\pi)^2}\, m_Z \sin 2\beta \sum_f N^f_C\, I^{3L}_f\, h^2_f\, B_0(m^2_{A^0}, m^2_f, m^2_f) \tag{77}$$

$$\Pi^{\tilde{\chi}^0}_{AZ} = \frac{i}{(4\pi)^2}\, 2\, g\, g_Z \sum_{k,l=1}^{4} F^0_{kl3}\, O''^L_{lk} \Big[m_{\tilde{\chi}^0_l}\, B_0 + (m_{\tilde{\chi}^0_l} - m_{\tilde{\chi}^0_k}) B_1 \Big](m^2_{A^0}, m^2_{\tilde{\chi}^0_l}, m^2_{\tilde{\chi}^0_k}) \tag{78}$$

$$\begin{aligned}\Pi^{\tilde{\chi}^+}_{AZ} = \frac{i}{(4\pi)^2}\, 2\, g\, g_Z \sum_{k,l=1}^{2} \Big[& \Big(F^+_{kl3}\, O'^L_{lk} - F^+_{lk3}\, O'^R_{lk} \Big) m_{\tilde{\chi}^+_l} (B_0 + B_1) \\ & + \Big(F^+_{kl3}\, O'^R_{lk} - F^+_{lk3}\, O'^L_{lk} \Big) m_{\tilde{\chi}^+_k}\, B_1 \Big](m^2_{A^0}, m^2_{\tilde{\chi}^+_l}, m^2_{\tilde{\chi}^+_k})\end{aligned} \tag{79}$$

$$\Pi^{\tilde{f}}_{AZ} = -\frac{1}{(4\pi)^2}\, 2\, g_Z \sum_f N^f_C\, z^{\tilde{f}}_{21}\, G^{\tilde{f}}_{123} \Big(B_0 + 2B_1 \Big)(m^2_{A^0}, m^2_{\tilde{f}_1}, m^2_{\tilde{f}_2}) \tag{80}$$

$$\Pi^H_{AZ} = \frac{i}{(4\pi)^2}\, \frac{g^2_Z\, m_Z}{4} \sum_{k=1}^{2} \sum_{l=3}^{4} A_{k,l-2}\, R_{k,l-2} (\beta - \alpha) \Big(B_0 + 2B_1 \Big)(m^2_{A^0}, m^2_{H^0_l}, m^2_{H^0_k}) \tag{81}$$

$$\Pi^Z_{AZ} = \frac{i}{(4\pi)^2}\, \frac{g^2_Z\, m_Z}{4} \sin(2\alpha - 2\beta) \sum_{k=1}^{2} (-1)^k \Big(B_0 - B_1 \Big)(m^2_{A^0}, m^2_{H^0_k}, m^2_Z) \tag{82}$$

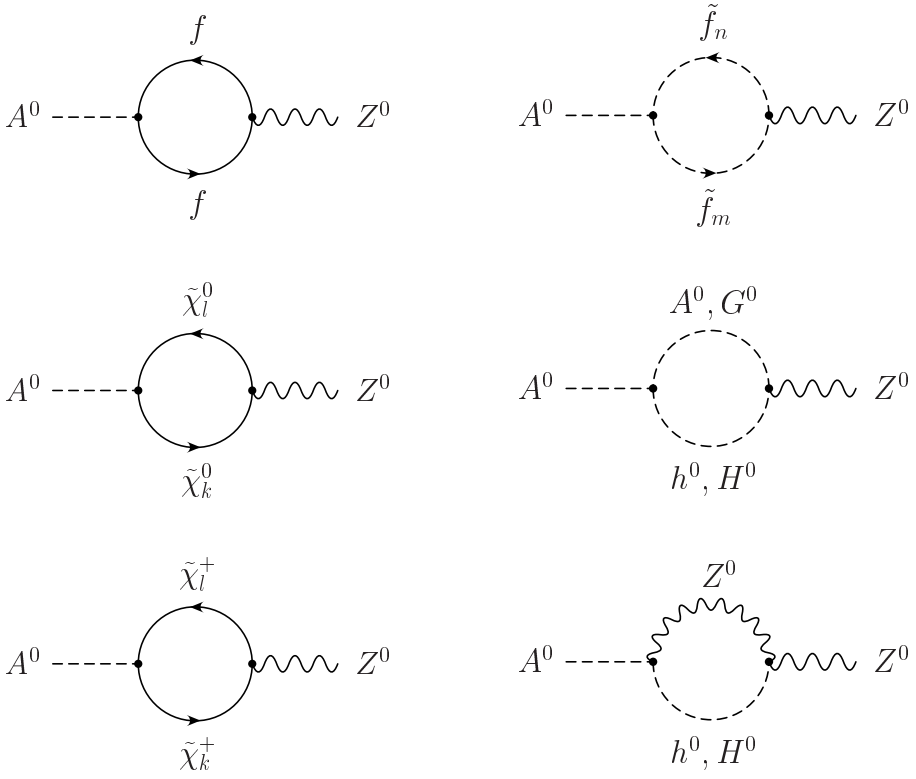

Figure 15: AZ–mixing self–energies

D.2 W^+ self–energies

For the calculation of the mass counter term of a gauge boson V ($V = W^\pm, Z^0$), $\delta m_V^2 = \Re\,\Pi_{VV}^T(m_V^2)$, we need the transverse part of the vector self–energy $\Pi_{VV}^T(k^2)$ from

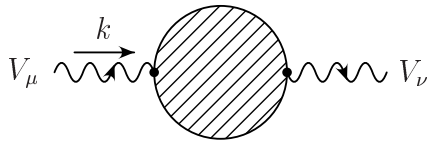

$$\mathcal{M} = -i\,\epsilon_\mu(k)\Big(g^{\mu\nu}\Pi_{VV}^T(k^2) + k^\mu k^\nu\,\Pi_{VV}^B(k^2)\Big)\epsilon_\nu^*(k)\,. \tag{83}$$

$$\left(\frac{\delta m_W}{m_W}\right)^{ff} = -\frac{1}{(4\pi)^2}\sum_{\text{gen.}} N_C^f\Bigg[h_{f_\uparrow}^2\sin^2\beta\,\frac{A_0(m_{f_\uparrow}^2)}{m_{f_\uparrow}^2} + h_{f_\downarrow}^2\cos^2\beta\,B_0(m_W^2, m_{f_\downarrow}^2, m_{f_\uparrow}^2) - \frac{g^2}{m_W^2}B_{00}(m_W^2, m_{f_\downarrow}^2, m_{f_\uparrow}^2) + \frac{g^2}{2}B_1(m_W^2, m_{f_\downarrow}^2, m_{f_\uparrow}^2)\Bigg] \tag{84}$$

$$\left(\frac{\delta m_W}{m_W}\right)^{\tilde{f}\tilde{f}} = -\frac{1}{(4\pi)^2}\,\frac{g^2}{m_W^2}\sum_{\text{gen.}} N_C^f\sum_{m,n=1}^{2}\left(R_{m1}^{\tilde{f}_\uparrow}R_{n1}^{\tilde{f}_\downarrow}\right)^2 B_{00}(m_W^2, m_{\tilde{f}_{\uparrow m}}^2, m_{\tilde{f}_{\downarrow n}}^2) \tag{85}$$

Here $f_\uparrow$ and $f_\downarrow$ denote up– and down–type (s)fermions of all three generations, respectively.

$$\left(\frac{\delta m_W}{m_W}\right)^{\tilde{f}} = \frac{1}{(4\pi)^2}\,\frac{g^2}{4m_W^2}\sum_{\text{gen.}} N_C^f \sum_{m=1}^{2}\left(R^{\tilde{f}}_{m1}\right)^2 A_0(m^2_{\tilde{f}_m}) \tag{86}$$

$$\left(\frac{\delta m_W}{m_W}\right)^{\tilde{\chi}} = \frac{1}{(4\pi)^2}\,\frac{g^2}{m_W^2}\sum_{k=1}^{2}\sum_{l=1}^{4}\Big[2\,O^L_{lk}\,O^R_{lk}\,m_{\tilde{\chi}^+_k}\,m_{\tilde{\chi}^0_l}\,B_0 - \Big((O^L_{lk})^2+(O^R_{lk})^2\Big)\times \Big(m_W^2\,B_1 + m^2_{\tilde{\chi}^0_l}\,B_0 + A_0(m^2_{\tilde{\chi}^+_k}) - 2\,B_{00}\Big)\Big](m_W^2, m^2_{\tilde{\chi}^0_l}, m^2_{\tilde{\chi}^+_k}) \tag{87}$$

$$\left(\frac{\delta m_W}{m_W}\right)^{HH} = -\frac{1}{(4\pi)^2}\,\frac{g^2}{2m_W^2}\Big[\sum_{k,l=1}^{2}\Big(R_{lk}(\alpha-\beta)\Big)^2 B_{00}(m_W^2, m^2_{H^+_l}, m^2_{H^0_k}) + B_{00}(m_W^2, m^2_{H^+}, m^2_{A^0}) + B_{00}(m_W^2, m^2_{G^+}, m^2_{G^0})\Big] \tag{88}$$

$$\left(\frac{\delta m_W}{m_W}\right)^{H} = \frac{1}{(4\pi)^2}\,\frac{g^2}{8m_W^2}\left(\sum_{k=1}^{4} A_0(m^2_{H^0_k}) + 2\sum_{k=1}^{2} A_0(m^2_{H^+_k})\right) \tag{89}$$

$$\left(\frac{\delta m_W}{m_W}\right)^{VS} = \frac{1}{(4\pi)^2}\,\frac{g^2}{2}\Big[\sum_{k=1}^{2}\Big(R_{2k}(\alpha-\beta)\Big)^2 B_0(m_W^2, m^2_{H^0_k}, m_W^2) + s_W^2\,B_0(m_W^2, m_W^2, \lambda^2) + s_W^2 t_W^2\,B_0(m_W^2, m_W^2, m_Z^2)\Big] \tag{90}$$

$$\left(\frac{\delta m_W}{m_W}\right)^{VV+V+\text{ghost}} = -\frac{1}{(4\pi)^2}\,\frac{g^2}{2m_W^2}\Big[s_W^2\Big(8B_{00}+7m_W^2B_0+2m_W^2B_1\Big)(m_W^2, m_W^2, \lambda^2) + c_W^2\Big(8B_{00}+7m_W^2B_0+2m_W^2B_1\Big)(m_W^2, m_W^2, m_Z^2) - s_W^2 A_0(\lambda^2) - c_W^2 A_0(m_Z^2) - 3A_0(m_W^2)\Big] \tag{91}$$

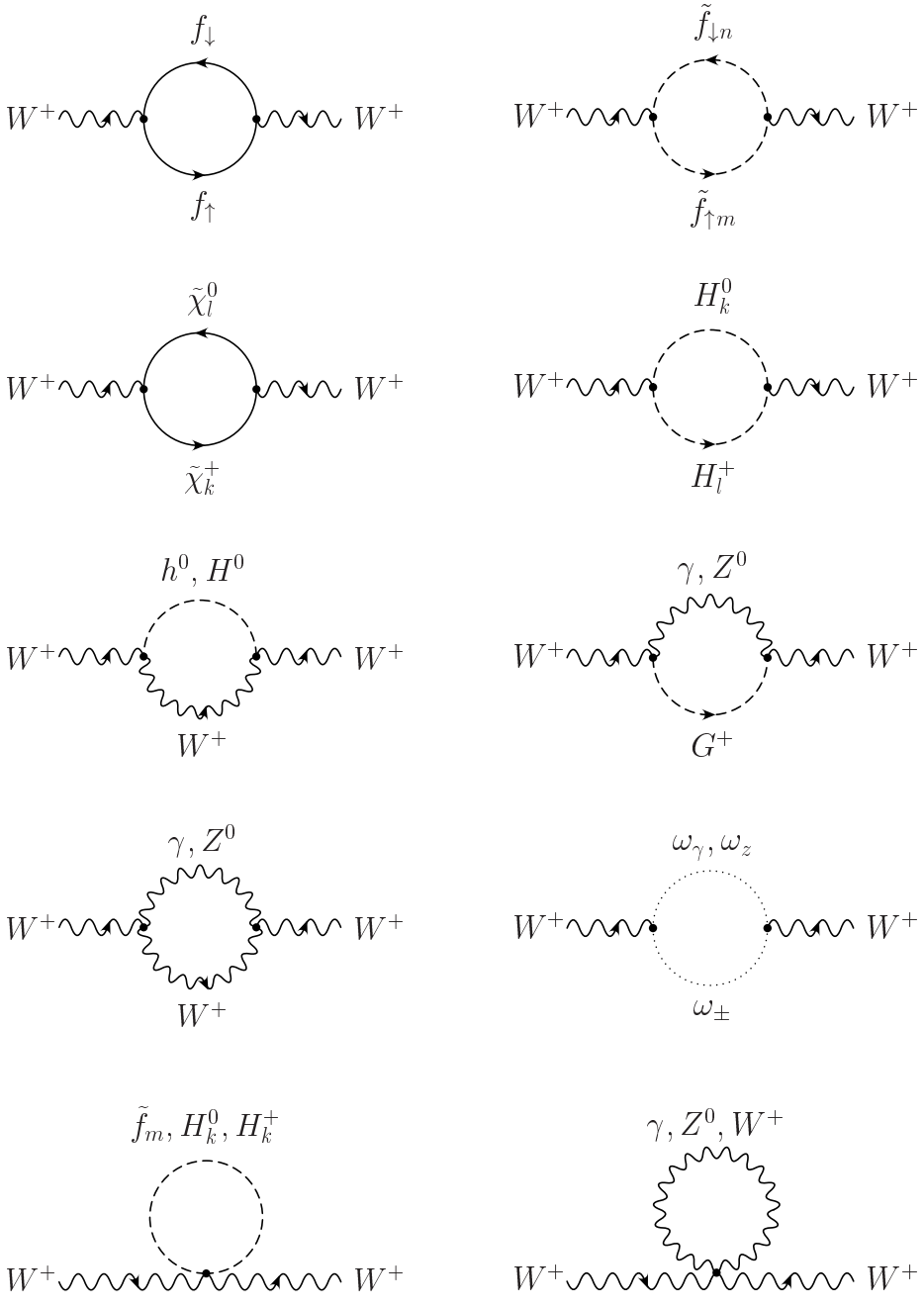

Figure 16: W^+ self–energies

D.3 Z^0 self–energies

Accordingly to eq. (83) the mass counter term contributions to the gauge boson Z^0 are:

$$\left(\frac{\delta m_Z}{m_Z}\right)^{ff} = \frac{1}{(4\pi)^2}\frac{g_Z^2}{m_Z^2}\sum_f N_C^f\Big[2\,C_L^f\,C_R^f\,m_f^2\,B_0 - \Big((C_L^f)^2+(C_R^f)^2\Big)\times \Big(A_0(m_f^2)+m_f^2\,B_0 - 2B_{00} + m_Z^2\,B_1\Big)\Big]\Big(m_Z^2,m_f^2,m_f^2\Big) \quad (92)$$

$$\left(\frac{\delta m_Z}{m_Z}\right)^{\tilde f\tilde f} = -\frac{1}{(4\pi)^2}\frac{2\,g_Z^2}{m_Z^2}\sum_f N_C^f\sum_{m,n=1}^{2}\Big(z^{\tilde f}_{mn}\Big)^2\,B_{00}(m_Z^2,m^2_{\tilde f_m},m^2_{\tilde f_n}) \quad (93)$$

$$\left(\frac{\delta m_Z}{m_Z}\right)^{\tilde f} = \frac{1}{(4\pi)^2}\frac{g_Z^2}{m_Z^2}\sum_f N_C^f\sum_{m=1}^{2}\Big(\Big(C_L^f\,R^{\tilde f}_{m1}\Big)^2+\Big(C_R^f\,R^{\tilde f}_{m2}\Big)^2\Big)A_0(m^2_{\tilde f_m}) \quad (94)$$

$$\left(\frac{\delta m_Z}{m_Z}\right)^{\tilde\chi^0} = -\frac{1}{(4\pi)^2}\frac{g_Z^2}{m_Z^2}\sum_{k,l=1}^{4}\Big(O''_{kl}\Big)^2\Big[(m_{\tilde\chi^0_k}+m_{\tilde\chi^0_l})m_{\tilde\chi^0_l}\,B_0 + m_Z^2\,B_1 + A_0(m^2_{\tilde\chi^0_k}) - 2\,B_{00}\Big](m_Z^2,m^2_{\tilde\chi^0_k},m^2_{\tilde\chi^0_l}) \quad (95)$$

$$\left(\frac{\delta m_Z}{m_Z}\right)^{\tilde\chi^+} = \frac{1}{(4\pi)^2}\frac{g_Z^2}{m_Z^2}\sum_{k,l=1}^{2}\Big[2\,O'^L_{kl}\,O'^R_{kl}\,m_{\tilde\chi^+_k}\,m_{\tilde\chi^+_l}\,B_0 - \Big((O'^L_{kl})^2+(O'^R_{kl})^2\Big)\times \Big(m_Z^2\,B_1 + m^2_{\tilde\chi^+_k}\,B_0 + A_0(m^2_{\tilde\chi^+_k}) - 2\,B_{00}\Big)\Big](m_Z^2,m^2_{\tilde\chi^+_k},m^2_{\tilde\chi^+_l}) \quad (96)$$

$$\left(\frac{\delta m_Z}{m_Z}\right)^{HH} = -\frac{1}{(4\pi)^2}\frac{g_Z^2}{2m_Z^2}\Big[\sum_{k=1}^{2}\sum_{l=3}^{4}\Big(R_{k,l-2}(\beta-\alpha)\Big)^2\,B_{00}(m_Z^2,m^2_{H^0_k},m^2_{H^0_l}) + \cos^2(2\theta_W)\sum_{k=1}^{2}B_{00}(m_Z^2,m^2_{H^+_k},m^2_{H^+_k})\Big] \quad (97)$$

$$\left(\frac{\delta m_Z}{m_Z}\right)^{H} = \frac{1}{(4\pi)^2}\frac{g_Z^2}{8m_Z^2}\Big[\sum_{k=1}^{4}A_0(m^2_{H^0_k}) + 2\cos^2(2\theta_W)\sum_{k=1}^{2}A_0(m^2_{H^+_k})\Big] \quad (98)$$

$$\left(\frac{\delta m_Z}{m_Z}\right)^{VS} = \frac{1}{(4\pi)^2}\Big(\frac{g_Z^2}{2}\sin^2(\alpha-\beta)\,B_0(m_Z^2,m^2_{h^0},m_Z^2) + \frac{g_Z^2}{2}\cos^2(\alpha-\beta)\times B_0(m_Z^2,m^2_{H^0},m_Z^2) + g^2\,s_W^4\,B_0(m_Z^2,m_W^2,m^2_{G^+})\Big) \quad (99)$$

$$\left(\frac{\delta m_Z}{m_Z}\right)^{WW+W+\text{ghost}} = -\frac{1}{(4\pi)^2}\frac{g^2c_W^2}{m_Z^2}\Big[4B_{00}+m_W^2B_0+\frac{5}{2}m_Z^2B_0+m_Z^2B_1 - 2A_0(m_W^2)\Big](m_Z^2,m_W^2,m_W^2) \quad (100)$$

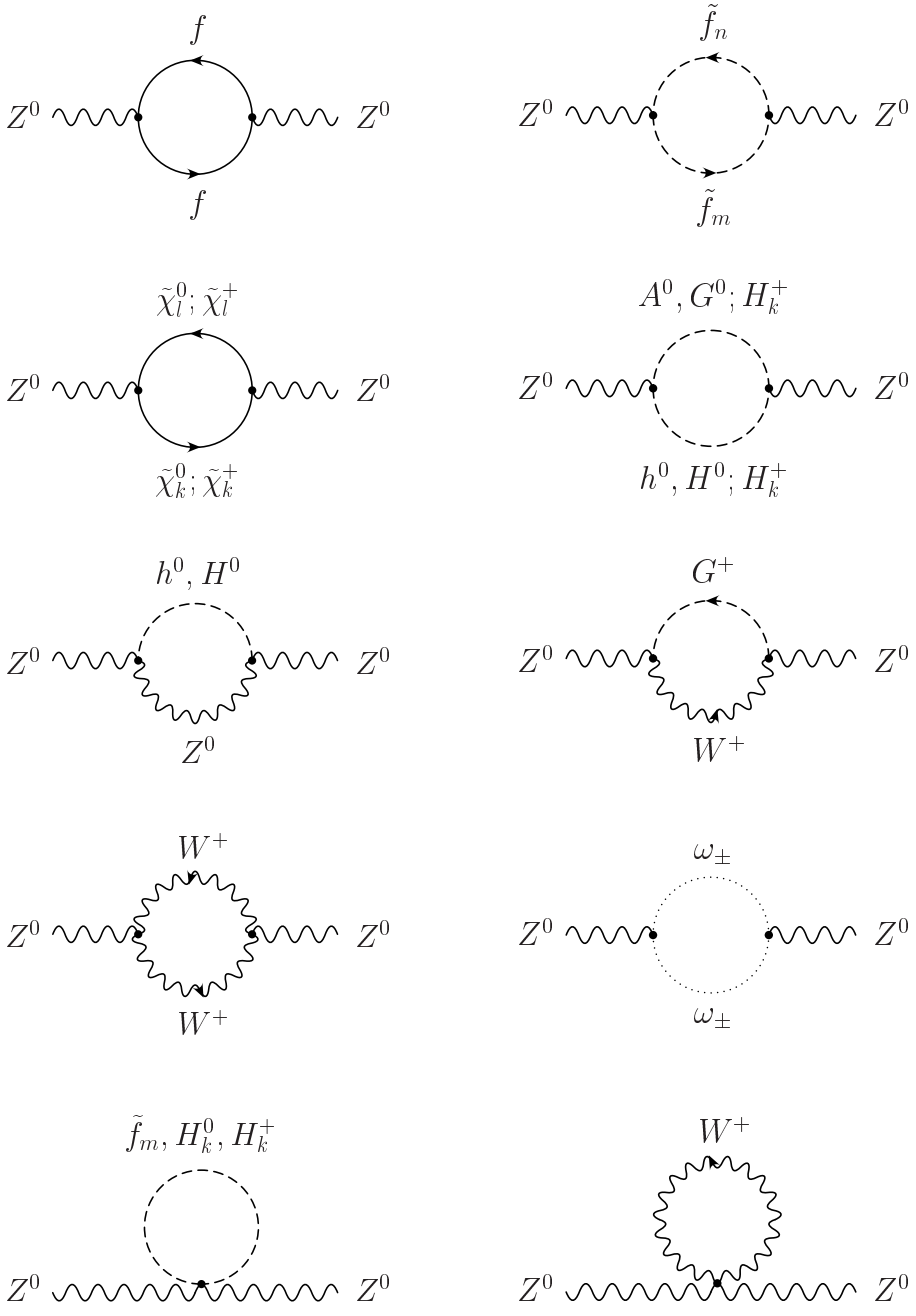

Figure 17: Z^0 self–energies

D.4 Fermion self–energies

In our notation, the fermion self–energy is defined by

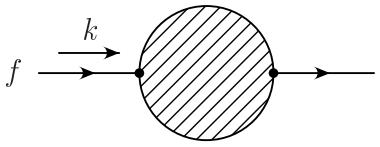

$$\mathcal{M} = i\,\bar{u}(k)\,\Pi(k)\,u(k)$$

with

$$\Pi(k) \;=\; \not{k}\,P_L\,\Pi^L(k) + \not{k}\,P_R\,\Pi^R(k) + \Pi^{SL}(k)P_L + \Pi^{SR}(k)P_R\,. \tag{101}$$

Thus the counter term for quarks and leptons is given by

$$\delta m_f \;=\; \frac{1}{2}\,\Re\left[m_f\left(\Pi^L(m_f) + \Pi^R(m_f)\right) + \Pi^{SL}(m_f) + \Pi^{SR}(m_f)\right]\,. \tag{102}$$

Note that for quarks and leptons (contrary to charginos), the left– and right–handed scalar parts of $\Pi(k)$ are equal, $\Pi^{SL}(k) = \Pi^{SR}(k)$. The single contributions to δm_f are as follows:

$$\left(\frac{\delta m_f}{m_f}\right)^{fH_k^0} \;=\; \frac{1}{(4\pi)^2}\left[\sum_{k=1}^{2}(s_k^f)^2\Big(B_0 - B_1\Big) + \sum_{k=3}^{4}(s_k^f)^2\,\Big(B_0 + B_1\Big)\right](m_f^2, m_f^2, m_{H_k^0}^2) \tag{103}$$

$$\left(\frac{\delta m_f}{m_f}\right)^{f'H_k^+} \;=\; -\frac{1}{(4\pi)^2}\sum_{k=1}^{2}\left[\frac{1}{2}\Big((y_k^f)^2 + (y_k^{f'})^2\Big)B_1 - \frac{m_{f'}}{m_f}\,y_k^f\,y_k^{f'}\,B_0\right](m_f^2, m_{f'}^2, m_{H_k^+}^2) \tag{104}$$

$$\left(\frac{\delta m_f}{m_f}\right)^{\tilde{f}\tilde{\chi}^0} \;=\; -\frac{1}{(4\pi)^2}\sum_{m=1}^{2}\sum_{k=1}^{4}\left[\frac{1}{2}\Big((a_{mk}^{\tilde{f}})^2 + (b_{mk}^{\tilde{f}})^2\Big)B_1 - \frac{m_{\tilde{\chi}_k^0}}{m_f}\,a_{mk}^{\tilde{f}}b_{mk}^{\tilde{f}}\,B_0\right](m_f^2, m_{\tilde{\chi}_k^0}^2, m_{\tilde{f}_m}^2) \tag{105}$$

$$\left(\frac{\delta m_f}{m_f}\right)^{\tilde{f}'\tilde{\chi}^+} \;=\; -\frac{1}{(4\pi)^2}\sum_{m=1}^{2}\sum_{k=1}^{2}\left[\frac{1}{2}\Big((k_{mk}^{\tilde{f}'})^2 + (l_{mk}^{\tilde{f}'})^2\Big)B_1 - \frac{m_{\tilde{\chi}_k^+}}{m_f}\,k_{mk}^{\tilde{f}'}\,l_{mk}^{\tilde{f}'}\,B_0\right](m_f^2, m_{\tilde{\chi}_k^+}^2, m_{\tilde{f}'_m}^2) \tag{106}$$

$$\left(\frac{\delta m_f}{m_f}\right)^{f\gamma} \;=\; -\frac{1}{(4\pi)^2}\,2(e_0e_f)^2\Big(B_0 - B_1\Big)(m_f^2, \lambda^2, m_f^2)$$

$$\left(\frac{\delta m_f}{m_f}\right)^{fZ^0} \;=\; -\frac{1}{(4\pi)^2}\,g_z^2\left[\Big((C_L^f)^2 + (C_R^f)^2\Big)B_1 + 4C_L^fC_R^f\,B_0\right](m_f^2, m_f^2, m_z^2) \tag{107}$$

$$\left(\frac{\delta m_f}{m_f}\right)^{f'W^+} \;=\; -\frac{1}{(4\pi)^2}\,\frac{g^2}{2}\,B_1(m_f^2, m_{f'}^2, m_W^2) \tag{108}$$

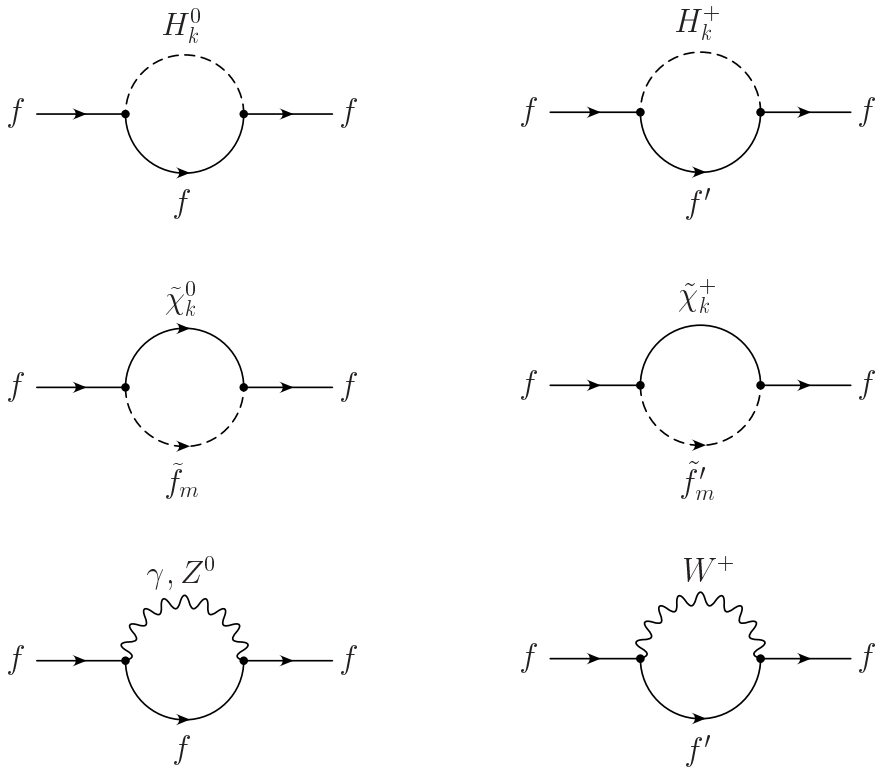

Figure 18: Fermion self–energies

D.5 Chargino self–energies

Since the higgsino mass parameter μ is fixed in the chargino sector, the counter term $\delta\mu$ reads [20, 21]

$$\delta\mu \;=\; \delta X_{22} \;=\; \frac{1}{2}\sum_{k,l=1}^{2} U_{k2}V_{l2}\Big(\Pi^L_{lk}\, m_{\tilde{\chi}^+_k} + \Pi^R_{kl}\, m_{\tilde{\chi}^+_l} + \Pi^{SL}_{kl} + \Pi^{SR}_{lk}\Big) \tag{109}$$

with the chargino self–energies $\Pi_{kl} = \Pi_{kl}(m^2_{\tilde{\chi}^+_l})$. U and V are two real 2×2 matrices which diagonalize the chargino mass matrix,

$$U\,X\,V^T \;=\; M_D \;=\; \begin{pmatrix} m_{\tilde{\chi}^+_1} & 0 \\ 0 & m_{\tilde{\chi}^+_2} \end{pmatrix}.$$

The single left– and right–handed parts of Π_{kl} can be found by comparing the coefficients accordingly to eq. (101).

fermion–sfermion contribution:

$$\Pi^{L,f}_{ij}(k^2) \;=\; -\frac{1}{(4\pi)^2}\sum_f N^f_C \sum_{m=1}^{2}\Big[k^{\tilde{f}_\downarrow}_{mi}k^{\tilde{f}_\downarrow}_{mj}\,B_1\Big(k^2, m^2_{f_\uparrow}, m^2_{\tilde{f}_{\downarrow m}}\Big) + l^{\tilde{f}_\uparrow}_{mi}l^{\tilde{f}_\uparrow}_{mj}\,B_1\Big(k^2, m^2_{f_\downarrow}, m^2_{\tilde{f}_{\uparrow m}}\Big)\Big]$$

$$
\begin{aligned}
\Pi_{ij}^{R,f}(k^2) &= -\frac{1}{(4\pi)^2}\sum_f N_C^f \sum_{m=1}^{2}\Big[l_{mi}^{\tilde{f}_\downarrow} l_{mj}^{\tilde{f}_\downarrow} B_1\Big(k^2, m_{f_\uparrow}^2, m_{\tilde{f}_{\downarrow m}}^2\Big) + k_{mi}^{\tilde{f}_\uparrow} k_{mj}^{\tilde{f}_\uparrow} B_1\Big(k^2, m_{f_\downarrow}^2, m_{\tilde{f}_{\uparrow m}}^2\Big)\Big] \\
\Pi_{ij}^{SL,f}(k^2) &= \frac{1}{(4\pi)^2}\sum_f N_C^f \sum_{m=1}^{2}\Big[m_{f_\uparrow} l_{mi}^{\tilde{f}_\downarrow} k_{mj}^{\tilde{f}_\downarrow} B_0\Big(k^2, m_{f_\uparrow}^2, m_{\tilde{f}_{\downarrow m}}^2\Big) + m_{f_\downarrow} k_{mi}^{\tilde{f}_\uparrow} l_{mj}^{\tilde{f}_\uparrow} \times \\
&\qquad\qquad B_0\Big(k^2, m_{f_\downarrow}^2, m_{\tilde{f}_{\uparrow m}}^2\Big)\Big] \\
\Pi_{ij}^{SR,f}(k^2) &= \frac{1}{(4\pi)^2}\sum_f N_C^f \sum_{m=1}^{2}\Big[m_{f_\uparrow} k_{mi}^{\tilde{f}_\downarrow} l_{mj}^{\tilde{f}_\downarrow} B_0\Big(k^2, m_{f_\uparrow}^2, m_{\tilde{f}_{\downarrow m}}^2\Big) + m_{f_\downarrow} l_{mi}^{\tilde{f}_\uparrow} k_{mj}^{\tilde{f}_\uparrow} \times \\
&\qquad\qquad B_0\Big(k^2, m_{f_\downarrow}^2, m_{\tilde{f}_{\uparrow m}}^2\Big)\Big]
\end{aligned}
\tag{110}
$$

Higgs/gaugino contribution:

$$
\begin{aligned}
\Pi_{ij}^{H_l^0}(k) &= -\frac{1}{(4\pi)^2} g^2 \sum_{k=1}^{2}\Bigg[\not{k}\sum_{l=1}^{4}\Big(F_{ikl}^{+}F_{jkl}^{+}P_L + F_{kil}^{+}F_{kjl}^{+}P_R\Big)B_1 \\
&\qquad -m_{\tilde{\chi}_k^+}\sum_{l=1}^{2}\Big(F_{kil}^{+}F_{jkl}^{+}P_L + F_{ikl}^{+}F_{kjl}^{+}P_R\Big)B_0 \\
&\qquad +m_{\tilde{\chi}_k^+}\sum_{l=3}^{4}\Big(F_{kil}^{+}F_{jkl}^{+}P_L + F_{ikl}^{+}F_{kjl}^{+}P_R\Big)B_0\Bigg]\Big(k^2, m_{\tilde{\chi}_k^+}^2, m_{H_l^0}^2\Big)
\end{aligned}
\tag{111}
$$

$$
\begin{aligned}
\Pi_{ij}^{H_l^+}(k) &= -\frac{1}{(4\pi)^2} g^2 \sum_{k=1}^{4}\sum_{l=1}^{2}\Big[\not{k}\Big(F_{ikl}^{R}F_{jkl}^{R}P_L + F_{ikl}^{L}F_{jkl}^{L}P_R\Big)B_1 \\
&\qquad -m_{\tilde{\chi}_k^0}\Big(F_{ikl}^{L}F_{jkl}^{R}P_L + F_{ikl}^{R}F_{jkl}^{L}P_R\Big)B_0\Big](k^2, m_{\tilde{\chi}_k^0}^2, m_{H_l^+}^2\Big)
\end{aligned}
\tag{112}
$$

$$
\Pi_{ij}^{\gamma}(k) = -\frac{1}{(4\pi)^2}\,2e^2\delta_{ij}\Big[\not{k}\,B_1 + 2m_{\tilde{\chi}_j^+}B_0\Big](k^2, m_{\tilde{\chi}_j^+}^2, \lambda^2) \tag{113}
$$

$$
\begin{aligned}
\Pi_{ij}^{Z^0}(k) &= -\frac{1}{(4\pi)^2}\,2\,g_Z^2\sum_{k=1}^{2}\Big[\not{k}\Big(O_{ik}^{\prime L}O_{kj}^{\prime L}P_L + O_{ik}^{\prime R}O_{kj}^{\prime R}P_R\Big)B_1 \\
&\qquad +2m_{\tilde{\chi}_k^+}\Big(O_{ik}^{\prime R}O_{kj}^{\prime L}P_L + O_{ik}^{\prime L}O_{kj}^{\prime R}P_R\Big)B_0\Big](k^2, m_{\tilde{\chi}_k^+}^2, m_Z^2\Big)
\end{aligned}
\tag{114}
$$

$$
\begin{aligned}
\Pi_{ij}^{W^+}(k) &= -\frac{1}{(4\pi)^2}\,2\,g^2\sum_{k=1}^{4}\Big[\not{k}\Big(O_{ki}^{L}O_{kj}^{L}P_L + O_{ki}^{R}O_{kj}^{R}P_R\Big)B_1 \\
&\qquad +2m_{\tilde{\chi}_k^0}\Big(O_{ki}^{R}O_{kj}^{L}P_L + O_{ki}^{L}O_{kj}^{R}P_R\Big)B_0\Big](k^2, m_{\tilde{\chi}_k^0}^2, m_W^2\Big)
\end{aligned}
\tag{115}
$$

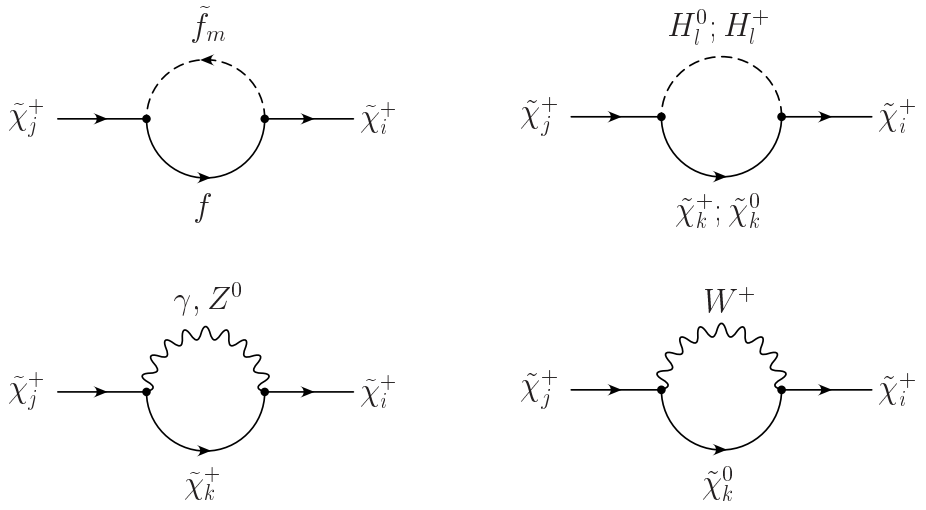

Figure 19: Chargino self–energies

D.6 Sfermion self–energies

For the fixing of the sfermion mixing angle $\theta_{\tilde{f}}$ we need the off–diagonal elements of the sfermion self–energies, $\Pi_{ij}^{\tilde{f}} = \Pi_{ij}^{\tilde{f}}(m^2_{\tilde{f}_j})$. In the following, $Y^f_{L/R}$ denotes the weak hypercharge, $Y^f_{L/R} = 2(I_f^{3L/R} - e_f)$. The short forms for various products of sfermion rotation matrices can be found in B. Additionally, we use the abbreviation $R^{\tilde{f}\hat{\tilde{f}}_D}_{ijkl} = R^{\tilde{f}}_{i1} R^{\tilde{f}}_{j1} R^{\hat{\tilde{f}}}_{k2} R^{\hat{\tilde{f}}}_{l2}$.

$$
\begin{aligned}
\Pi_{ij}^{\tilde{f},\tilde{\chi}} &= -\frac{1}{(4\pi)^2} \sum_{k=1}^{4} \Big[\Big(a^{\tilde{f}}_{ik} a^{\tilde{f}}_{jk} + b^{\tilde{f}}_{ik} b^{\tilde{f}}_{jk} \Big) \cdot \Big(A_0(m^2_{\tilde{\chi}^0_k}) + A_0(m_f^2) + (m^2_{\tilde{\chi}^0_k} + m_f^2 - m^2_{\tilde{f}_j})\, B_0 \Big) \\
&\qquad + \Big(a^{\tilde{f}}_{ik} b^{\tilde{f}}_{jk} + b^{\tilde{f}}_{ik} a^{\tilde{f}}_{jk} \Big) \cdot 2 m_{\tilde{\chi}^0_k} m_f B_0 \Big] (m^2_{\tilde{f}_j}, m^2_{\tilde{\chi}^0_k}, m_f^2) \\
&\quad -\frac{1}{(4\pi)^2} \sum_{k=1}^{2} \Big[\Big(k^{\tilde{f}}_{ik} k^{\tilde{f}}_{jk} + l^{\tilde{f}}_{ik} l^{\tilde{f}}_{jk} \Big) \cdot \Big(A_0(m^2_{\tilde{\chi}^+_k}) + A_0(m^2_{f'}) + (m^2_{\tilde{\chi}^+_k} + m^2_{f'} - m^2_{\tilde{f}_j})\, B_0 \Big) \\
&\qquad + \Big(k^{\tilde{f}}_{ik} l^{\tilde{f}}_{jk} + l^{\tilde{f}}_{ik} k^{\tilde{f}}_{jk} \Big) \cdot 2 m_{\tilde{\chi}^+_k} m_{f'} B_0 \Big] (m^2_{\tilde{f}_j}, m^2_{\tilde{\chi}^+_k}, m^2_{f'}) \qquad (116)
\end{aligned}
$$

$$
\begin{aligned}
\Pi_{ij}^{\tilde{f},H\tilde{f}} &= \frac{1}{(4\pi)^2} \sum_{k=1}^{4} \sum_{m=1}^{2} G^{\tilde{f}}_{mik}\, G^{\tilde{f}}_{jmk}\, B_0(m^2_{\tilde{f}_j}, m^2_{\tilde{f}_m}, m^2_{H^0_k}) \\
&\quad + \frac{1}{(4\pi)^2} \sum_{k=1}^{2} \sum_{m=1}^{2} G^{\tilde{f}'\tilde{f}}_{mik}\, G^{\tilde{f}\tilde{f}'}_{jmk}\, B_0(m^2_{\tilde{f}_j}, m^2_{\tilde{f}'_m}, m^2_{H^+_k}) \qquad (117) \\
\Pi_{ij}^{\tilde{f},\gamma\tilde{f}} &= -\frac{1}{(4\pi)^2} (e_0 e_f)^2 \delta_{ij} \Big[2A_0(\lambda^2) - A_0(m^2_{\tilde{f}_i}) + \Big(4m^2_{\tilde{f}_i} - \lambda^2 \Big) B_0(m^2_{\tilde{f}_i}, m^2_{\tilde{f}_i}, \lambda^2) \Big]
\end{aligned}
$$

(118)

$$\Pi_{ij}^{\tilde{f},\,Z\tilde{f}} = -\frac{1}{(4\pi)^2}\,g_Z^2\sum_{m=1}^{2} z_{mi}^{\tilde{f}} z_{jm}^{\tilde{f}}\Big[2A_0(m_Z^2) - A_0(m_{\tilde{f}_m}^2) + \Big(2m_{\tilde{f}_j}^2 + 2m_{\tilde{f}_m}^2 - m_Z^2\Big)\times B_0(m_{\tilde{f}_j}^2, m_{\tilde{f}_m}^2, m_Z^2)\Big] \quad (119)$$

$$\Pi_{ij}^{\tilde{f},\,W\tilde{f}'} = -\frac{1}{(4\pi)^2}\,\frac{g^2}{2} R_{i1}^{\tilde{f}} R_{j1}^{\tilde{f}}\sum_{m=1}^{2}\Big(R_{m1}^{\tilde{f}'}\Big)^2\Big[2A_0(m_W^2) - A_0(m_{\tilde{f}'_m}^2) + \Big(2m_{\tilde{f}_j}^2 + 2m_{\tilde{f}'_m}^2 - m_W^2\Big)\times B_0(m_{\tilde{f}_j}^2, m_{\tilde{f}'_m}^2, m_W^2)\Big] \quad (120)$$

$$\begin{aligned}\Pi_{ij}^{\tilde{f},\,\tilde{f}} &= \frac{1}{(4\pi)^2}\,h_f^2\sum_{m=1}^{2}\Big[N_C^f\Big(R_{jmmi}^{\tilde{f}} + R_{mijm}^{\tilde{f}}\Big) + R_{jimm}^{\tilde{f}} + R_{mmji}^{\tilde{f}}\Big]A_0(m_{\tilde{f}_m}^2)\\ &+\frac{1}{(4\pi)^2}\,g_Z^2\sum_{m=1}^{2}\Big\{\Big[\Big(\frac{1}{4} - (2I_f^{3L} - e_f)e_f s_W^2\Big)R_{jimm}^{\tilde{f}_L} + e_f^2 s_W^2 R_{jimm}^{\tilde{f}_R}\Big](N_C^f + 1)\\ &\quad +(I_f^{3L} - e_f)e_f s_W^2\Big[N_C^f\Big(R_{jimm}^{\tilde{f}} + R_{mmji}^{\tilde{f}}\Big) + R_{jmmi}^{\tilde{f}} + R_{mijm}^{\tilde{f}}\Big]\Big\}A_0(m_{\tilde{f}_m}^2)\end{aligned} \quad (121)$$

$$\begin{aligned}\Pi_{ij}^{\tilde{f},\,\tilde{f}'} &= \frac{1}{(4\pi)^2}\sum_{m=1}^{2}\Big(h_f^2\,R_{mmji}^{\tilde{f}'\tilde{f}_D} + h_{f'}^2\,R_{jimm}^{\tilde{f}\tilde{f}'_D}\Big)A_0(m_{\tilde{f}'_m}^2)\\ &+\frac{1}{(4\pi)^2}\,\frac{g^2}{4}\sum_{m=1}^{2}\Big\{N_C^f\Big[\Big(t_W^2 Y_L^f Y_L^{f'} - 1\Big)R_{jimm}^{\tilde{f}\tilde{f}'_L} + t_W^2 Y_R^f Y_R^{f'}\,R_{jimm}^{\tilde{f}\tilde{f}'_R}\\ &\quad - Y_L^f Y_R^{f'}\,R_{jimm}^{\tilde{f}\tilde{f}'_D} - Y_L^{f'} Y_R^f R_{mmji}^{\tilde{f}'\tilde{f}_D}\Big] + 2R_{jimm}^{\tilde{f}\tilde{f}'_L}\Big\}A_0(m_{\tilde{f}'_m}^2)\end{aligned} \quad (122)$$

$$\begin{aligned}\Pi_{ij}^{\tilde{f},\,\hat{\tilde{f}}} &= \frac{1}{(4\pi)^2}N_C^{\hat{f}}\sum_{m=1}^{2}\Big[h_f h_{\hat{f}}\Big(R_{ijmm}^{\tilde{f}\hat{\tilde{f}}_F} + R_{jimm}^{\tilde{f}\hat{\tilde{f}}_F}\Big) + \frac{g^2}{4}R_{jimm}^{\tilde{f}\hat{\tilde{f}}_L}\Big]A_0(m_{\hat{\tilde{f}}_m}^2)\\ &+\frac{1}{(4\pi)^2}\,N_C^{\hat{f}}\,\frac{g'^2}{4}\sum_{m=1}^{2}\Big[Y_L^f Y_L^{\hat{f}} R_{jimm}^{\tilde{f}\hat{\tilde{f}}_L} - Y_L^f Y_R^{\hat{f}}\,R_{jimm}^{\tilde{f}\hat{\tilde{f}}_D} - Y_L^{\hat{f}} Y_R^f\,R_{mmji}^{\hat{\tilde{f}}\tilde{f}_D}\\ &\quad + Y_R^f Y_R^{\hat{f}} R_{jimm}^{\tilde{f}\hat{\tilde{f}}_R}\Big]A_0(m_{\hat{\tilde{f}}_m}^2)\end{aligned} \quad (123)$$

$$\begin{aligned}\Pi_{ij}^{\tilde{f},\,\hat{\tilde{f}}'} &= -\frac{1}{(4\pi)^2}N_C^{\hat{f}}\,\frac{g^2}{4}\sum_{m=1}^{2}R_{jimm}^{\tilde{f}\hat{\tilde{f}}'_L}A_0(m_{\hat{\tilde{f}}'_m}^2)\\ &+\frac{1}{(4\pi)^2}\,N_C^{\hat{f}}\,\frac{g'^2}{4}\sum_{m=1}^{2}\Big[Y_L^f Y_L^{\hat{f}'} R_{jimm}^{\tilde{f}\hat{\tilde{f}}'_L} - Y_L^f Y_R^{\hat{f}'}\,R_{jimm}^{\tilde{f}\hat{\tilde{f}}'_D} - Y_L^{\hat{f}'} Y_R^f\,R_{mmji}^{\hat{\tilde{f}}'\tilde{f}_D}\\ &\quad + Y_R^f Y_R^{\hat{f}'} R_{jimm}^{\tilde{f}\hat{\tilde{f}}'_R}\Big]A_0(m_{\hat{\tilde{f}}'_m}^2)\end{aligned} \quad (124)$$

The contributions from first and second generation sfermions, $\tilde{F}_m$, are given by

$$\begin{aligned} \Pi_{ij}^{\tilde{f},\tilde{F}} &= \Pi_{ij}^{\tilde{f},\hat{\tilde{f}}}(\hat{f} \to F)\,, \qquad & \Pi_{ij}^{\tilde{f},\hat{\tilde{F}}} &= \Pi_{ij}^{\tilde{f},\hat{\tilde{f}}}(\hat{f} \to \hat{F})\,, \\ \Pi_{ij}^{\tilde{f},\tilde{F}'} &= \Pi_{ij}^{\tilde{f},\hat{\tilde{f}}'}(\hat{f}' \to F')\,, \qquad & \Pi_{ij}^{\tilde{f},\hat{\tilde{F}}'} &= \Pi_{ij}^{\tilde{f},\hat{\tilde{f}}'}(\hat{f}' \to \hat{F}')\,, \end{aligned} \tag{125}$$

where the sub–/superscript $\tilde{F}$ denotes values belonging to first and second generation scalar fermions with same isospin as $\tilde{f}$ (e. g. $\tilde{F}_1 = \{\tilde{u}_1, \tilde{c}_1\}$ for the stop case, ...), $\tilde{F}'$ sfermions with different isospin etc.

$$\begin{aligned} \Pi_{ij}^{\tilde{f},H} &= \frac{1}{(4\pi)^2}\,\frac{1}{2}\sum_{k=1}^{4}\Big[h_f^2\, c_{kk}^{\tilde{f}}\,\delta_{ij} + g^2\, e_{ij}^{\tilde{f}}\left(c_{kk}^{\tilde{b}} - c_{kk}^{\tilde{t}}\right)\Big] A_0(m^2_{H_k^0}) \\ &\quad + \frac{1}{(4\pi)^2}\sum_{k=1}^{2}\Big[h_{f'}^2\, d_{kk}^{\tilde{f}'}\, R_{i1}^{\tilde{f}} R_{j1}^{\tilde{f}} + h_f^2\, d_{kk}^{\tilde{f}}\, R_{i2}^{\tilde{f}} R_{j2}^{\tilde{f}} + g^2\, f_{ij}^{\tilde{f}}\left(d_{kk}^{\tilde{b}} - d_{kk}^{\tilde{t}}\right)\Big] A_0(m^2_{H_k^+}) \end{aligned} \tag{126}$$

$$\begin{aligned} \Pi_{ij}^{\tilde{f},V} &= \frac{1}{(4\pi)^2}\,4\,(e_0 e_f)^2 \delta_{ij} A_0(\lambda^2) + \frac{1}{(4\pi)^2}\,2\,g^2 R_{i1}^{\tilde{f}} R_{j1}^{\tilde{f}} A_0(m_W^2) \\ &\quad + \frac{1}{(4\pi)^2}\,4\,g_z^2\Big[\left(C_L^f\right)^2 R_{i1}^{\tilde{f}} R_{j1}^{\tilde{f}} + \left(C_R^f\right)^2 R_{i2}^{\tilde{f}} R_{j2}^{\tilde{f}}\Big] A_0(m_Z^2) \end{aligned} \tag{127}$$

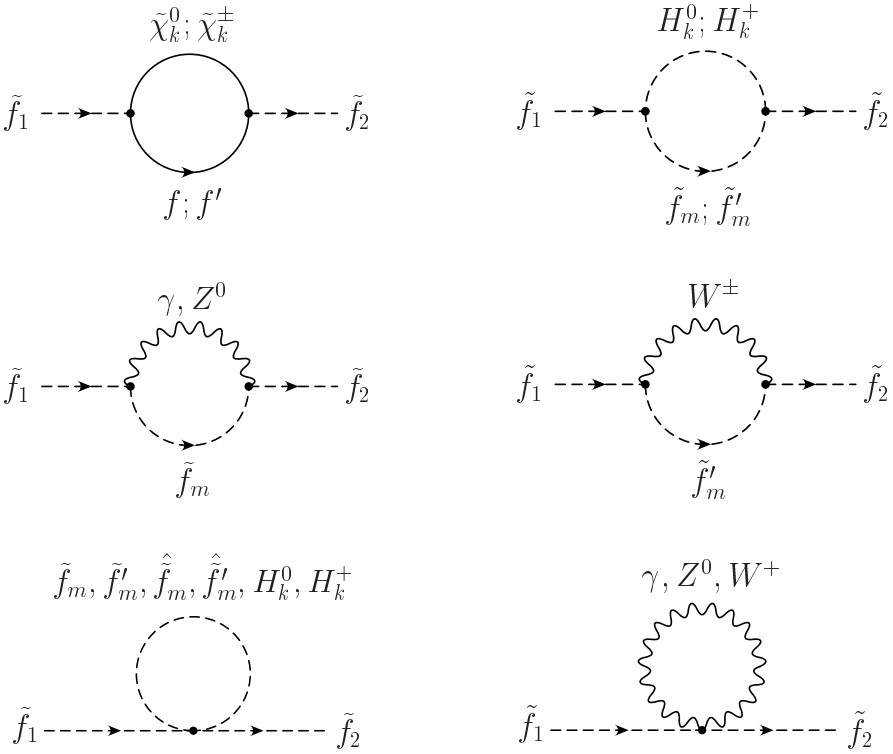

Figure 20: Off–diagonal Sfermion self–energies

References

[1] CERN–EP/2003-011, submitted to Phys. Lett. B.

[2] J. F. Gunion, H. E. Haber, Nucl. Phys B **272** (1986) 1; B **402** (1993) 567 (E).

[3] J. F. Gunion, H. E. Haber, G. L. Kane and S. Dawson, The Higgs Hunter's Guide, Addison-Wesley (1990).

[4] H. Baer, D. Dicus, M. Drees, and X. Tata, Phys. Rev. D **36** (1987) 1363;
J. F. Gunion and H. E. Haber, Nucl. Phys. B **307** (1988) 445;
J. F. Gunion and H. E. Haber, Nucl. Phys. B **402** (1993) 569(E);
K. Griest and H. E. Haber, Phys. Rev. D **37** (1988) 719.

[5] A. Djouadi, J. Kalinowski, and P. M. Zerwas, Z. Phys. C **57** (1993) 569;
A. Djouadi, P. Janot, J. Kalinowski, and P. M. Zerwas, Phys. Lett. B **376** (1996) 220;
A. Djouadi, J. Kalinowski, P. Ohmann, and P. M. Zerwas, Z. Phys. C **74** (1997) 93;
A. Djouadi, Mod. Phys. Lett. A **14** (1999) 359;
G. Bélanger, F. Boudjema, F. Donato, R. Godbole, and S. Rosier-Lees, Nucl. Phys. B **581** (2000) 3.

[6] A. Bartl, K. Hidaka, Y. Kizukuri, T. Kon and W. Majerotto, Phys. Lett **315** (1993) 360;
A. Djouadi, J. Kalinowski, P. Ohmann, P.M. Zerwas, Z. Phys. C **74** (1997) 93.

[7] A. Bartl, H.Eberl, K. Hidaka, T. Kon W. Majerotto and Y. Yamada, Phys. Lett **378** (1996) 167 and references therein.

[8] A. Bartl, H. Eberl, K. Hidaka, T. Kon, W. Majerotto and Y. Yamada, Phys. Lett. B **402** (1997) 303.

[9] A. Arhrib, A. Djouadi, W. Hollik, C. Jünger, Phys. Rev. D **57** (1998) 5860.

[10] H. Eberl, M. Kincel, W. Majerotto and Y. Yamada, Nucl. Phys. B **625** (2002) 372.

[11] R. Y. Zhang et al., Phys. Rev. D **65** (2002) 075018.

[12] C. Weber, H. Eberl and W. Majerotto, hep-ph/0305250, to be published in Phys. Lett. B.

[13] R. Hempfling, Phys. Rev. D **49** (1994) 6168;
L.J. Hall, R. Rattazzi, and U. Sarid, Phys. Rev. D **50** (1994) 7048;
M. Carena, M. Olechowski, S. Pokorski, and C.E.M. Wagner, Nucl. Phys. B **426** (1994) 269;
D.M. Pierce, J.A. Bagger, K. Matchev, and R. Zhang, Nucl. Phys. B **491** (1997) 3.

[14] H. Eberl, K. Hidaka, S. Kraml, W. Majerotto and Y. Yamada, Phys. Rev. D **62** (2000) 055006.

[15] E. Braaten and J.P. Leveille, Phys. Rev. D **22** (1980) 715;
M. Drees and K. Hikasa, Phys. Lett. B **240** (1990) 455; **262** (1991) 497 (E);
A. Méndez and A. Pomarol, Phys. Lett. B **252** (1990) 461.

[16] S.G. Gorishny, A.L. Kataev, S.A. Larin, and L.R. Surguladze, Mod. Phys. Lett. **A5** (1990) 2703; Phys. Rev. D **43** (1991) 1633;
A. Djouadi, M. Spira, and P.M. Zerwas, Z. Phys. C **70** (1996) 427;
A. Djouadi, J. Kalinowski, and M. Spira, Comput. Phys. Commun. **108** (1998) 56;
M. Spira, Fortschr. Phys. **46** (1998) 203.

[17] M. Carena, S. Mrenna, and C.E.M. Wagner, Phys. Rev. D **60** (1999) 075010; Phys. Rev. D **62** (2000) 055008.

[18] P.H. Chankowski and S. Pokorski, hep-ph/9707497, in *Perspectives on Supersymmetry*, ed. by G. L. Kane (World Scientific, 1997);
K.S. Babu and C. Kolda, Phys. Lett. B **451** (1999) 77.

[19] J. Guasch, J. Solà, and W. Hollik, Phys. Lett. B **437** (1998) 88;
H. Eberl, S. Kraml, and W. Majerotto, JHEP **9905** (1999) 016.

[20] H. Eberl, M. Kincel, W. Majerotto and Y. Yamada, Phys. Rev. D **64** (2001) 115013.

[21] W. Öller, H. Eberl, W. Majerotto and C. Weber, hep-ph/0304006, to be published in Eur. Phys. J. C.

[22] P. H. Chankowski, S. Pokorski, J. Rosiek, Phys. Lett. B **274** (1992) 191; Nucl. Phys. B **423** (1994) 437; 497;
A. Dabelstein, Z. Phys. C **67** (1995) 495; Nucl. Phys. B **456** (1995) 25.

[23] G. 't Hooft and M. Veltman, Nucl. Phys. B **153** (1979) 365;
G. Passarino and M. Veltman, Nucl. Phys. B **160** (1979) 151.

[24] A. Denner, Fortschr. Phys. **41** (1993) 307.